R. & M. No. 3573

R. & M. No. 3573

MINISTRY OF TECHNOLOGY

AERONAUTICAL RESEARCH COUNCIL
REPORTS AND MEMORANDA

The Formulation of an Influence-Coefficient Method for Determining Static Aeroelastic Effects, and its Application to a Slender Aircraft in Symmetric Flight at M = 2·2

By A. S. TAYLOR, M.Sc., A.F.R.Ae.S. and D. J. ECKFORD, B.Sc., A.F.I.M.A.
Structures Dept., R.A.E., Farnborough

LONDON: HER MAJESTY'S STATIONERY OFFICE
1969
PRICE £1 2*s.* 6*d.* NET

The Formulation of an Influence-Coefficient Method for Determining Static Aeroelastic Effects, and its Application to a Slender Aircraft in Symmetric Flight at M = 2·2

By A. S. TAYLOR, M.Sc., A.F.R.Ae.S. and D. J. ECKFORD, B.Sc., A.F.I.M.A.
Structures Dept., R.A.E., Farnborough

Reports and Memoranda No. 3573*
September, 1967

Summary.

This Report presents a matrix formulation of a method which employs influence coefficients to solve static aeroelastic problems. Linear structural characteristics are assumed and the aerodynamic loading, including that due to elastic deformation, is assumed to be compounded from a linear combination of 'elementary' distributions. Details of the method are here considered only for symmetric flight cases, though in essence it is universally applicable.

The method has been applied to a 'Concorde'-like supersonic transport aircraft in symmetric flight at $M = 2{\cdot}2$. Linearised supersonic theory has been used to derive the load due to elastic deformation. Results are presented for the incidences and elevator angles to trim and to sustain quasi-steady manoeuvres, for the longitudinal distributions of shear force and bending moment, and for the elastic deformation acquired.

The potentialities of the method are considered sufficient to justify the expenditure of the further effort which is necessary to develop it into a fully automated design procedure of wide applicability.

CONTENTS

*Replaces R.A.E. Tech. Report No. 67 237 (A.R.C. 30 059).

---

1. *Introduction.*

In Part I of R. & M. 3426[1] one of the present authors, A. S. Taylor, and W. F. W. Urich developed an approximate method of estimating the effects of aeroelasticity on the longitudinal trim and quasi-steady manoeuvrability of slender aircraft; in Part II of the same Report Taylor extended the investigation to include the estimation of the associated effects on the longitudinal distributions of shear force and bending moment. For this work it was assumed that, structurally, the aircraft behaved as a 'free-free' beam, subject only to longitudinal bending, and that the total chordwise aerodynamic loading (including

that due to elastic camber) varied linearly with local incidence and with elevator deflection, and was thus calculable by superposition of a number of 'elementary' distributions. This two-dimensional approach was conceived at an early stage of the exploratory investigations into the suitability of the slender near-delta planform for supersonic transport aircraft. At that time attention was focused on the 'completely integrated' slender-wing configuration, for which the spanwise stiffness might well have been large enough to justify the assumption of beam-like behaviour. In the event, however, the layout adopted for the first Anglo-French supersonic transport aircraft ('Concorde') featured a discrete fuselage, in conjunction with a thin slender wing, and from the project studies of the British Aircraft Corporation and Sud Aviation it soon became apparent that for such a configuration the hypothesis of purely longitudinal bending would be untenable. It thus seemed desirable to formulate a three-dimensional counterpart of the two-dimensional method given in R. & M. 3426, so that proper account could be taken of the spanwise deformability in the estimation of steady and quasi-steady aeroelastic effects. For the development of such a method, a matrix formulation of the problem, employing structural and aerodynamic influence coefficients, was selected.

The two-dimensional method was, of course, inherently applicable only to aircraft of slender delta configuration. No such restriction need be applied in the development of a (linearised) three-dimensional method which should, in principle, be able to cope with a layout of any type, operating in any flow regime, for which there exists an appropriate theory to provide the aerodynamic influence matrix to be associated with the incremental incidences due to distortion. Thus, at the outset, the object has been to enunciate the basis of the theory and to develop a practical form of considerable generality (Section 2). Later (Section 3), in order to provide a numerical illustration of the method, the theory has been specialised for the case of a 'Concorde'-like slender aircraft flying at $M = 2{\cdot}2$, and the results of calculations are presented in Section 3.6. For this application much of the data was provided by the British Aircraft Corporation. In the derivation of the aerodynamic influence matrix to be associated with the elastic distortion, linearised supersonic-flow theory was employed, *via* the method of D. E. Lees[2].

At this juncture no attempt has been made to assess the accuracy of the various parts of the method, nor its overall accuracy. The intention has been to present a generalised formulation of the matrix approach to the problem, and to gain experience in its numerical application, while obtaining a qualitative (and perhaps roughly quantitative) assessment of the quasi-steady aeroelastic effects on longitudinal trim, manoeuvrability and loading of a slender supersonic transport aircraft in cruising flight.

In Section 4 some discussion of the state of development achieved by the present investigation is given, together with indications of the further work that would be necessary to establish the method as a routine design procedure, of general applicability. In the final discussion (Section 5) it is concluded that the expenditure of effort on such work, which would include the automation of many of the processes involved, would be justifiable. For, inasmuch as it provides a direct and 'exact' solution of an idealised problem, the present method is superior to those which involve iteration or assumed modes of deformation while, in an automated version, it should compare quite favourably with them as regards computational economy.

2. *Theoretical Basis.*

2.1. *Some Introductory Remarks.*

Before proceeding to the development of a 'three-dimensional' theory it may be worthwhile to recall the salient features of the 'two-dimensional' approach since some useful concepts from the latter may be carried over to the former.

As already remarked in the Introduction, it was assumed for the 'two-dimensional' work that, structurally, the aircraft behaved as a 'free-free' beam, subject only to longitudinal bending, and that the total chordwise aerodynamic loading (including that due to elastic camber) varied linearly with local incidence and with elevator deflection, and was thus calculable by superposition of a number of 'elementary' distributions. The various distributions, other than that due to elastic camber, could be independently specified in accordance with the best available experimental or theoretical data. For the specification of loading due to elastic camber it was necessary to employ a simple (linearised) theory and for the

numerical work of R. & M. 3426 slender-wing and piston theories were selected. The differential equation for the deflected beam could then be set up and solved on a digital computer in conjunction with the equations of overall equilibrium. The distributions of elastic camber, the incidences of the centreline chord and the elevator angles appropriate to the cases of trimmed level flight and of steady pull-up manoeuvres were thus obtained.

In the formulation of a 'three-dimensional' method which shall be applicable over a wide range of planforms (including those of low aspect ratio) the choice of flexibility influence coefficients as a means of expressing the deformability characteristics of the structure is a natural one which leads on to the idea of expressing the aerodynamic loading due to distortion also by means of influence coefficients. The general principles underlying the solution of steady aeroelastic problems by means of influence coefficients were discussed by Williams[3] as long ago as 1954, and he sketched in some details of their application to specific problems, including wing divergence and the determination of aileron rolling power and elevator power. Four years earlier E. G. Broadbent, in investigating the rolling power of a swept wing, had used rather special forms of structural influence coefficients[4]. These forms were employed by Foody and Reid, in conjunction with aerodynamic influence coefficients derived by Küchemann's modified lifting-line theory, in a routine computational technique for the estimation of loading (in subsonic flow) on deformable wings of arbitrary planform. They first described this technique in 1954 in a report of Short Brothers and Harland Ltd; an abridged version of this report was published by the Royal Aeronautical Society in 1955[5]. However, the present authors are not aware of any detailed matrix formulation of the trim and manoeuvrability problems which is generally available in published form, and it has therefore seemed worthwhile to present such a formulation here.

2.2. *General Outline of the Method.*

The general outline of the theory is given below for symmetric flight conditions. The theory is not inherently so restricted and the principles governing its extension to asymmetric conditions are obvious. So long as any asymmetric case can be regarded as a planar problem, at least for a particular component, the method for symmetric cases can be applied with few changes other than in notation and interpretation of certain terms. However, in the case of completely general motion, involving significant deformations of the whole aircraft under a loading which has components in and normal to the plane of symmetry, the practical difficulties would be considerable.

An aircraft in a particular steady (or quasi-steady) symmetric flight condition is subject to distributed aerodynamic, inertial and gravitational loadings, and loads due to the propulsion system. These may all be resolved into components in and normal to a datum plane which lies near and approximately parallel to the wing. For simplicity it will be assumed that all propulsion system loads act in this plane and that, in common with all other load components in the plane, they cause negligible distortion of the aircraft structure. For our purposes, therefore, we may hereafter consider the aircraft as subject to a self-equilibrating distributed loading acting normally to the datum plane. This will have caused a deformation of the structure and, in particular, the streamwise slope at any point on the lifting surfaces will have been changed by an amount which we term *elastic incidence*. The lifting surfaces as a whole may be said to have acquired *elastic warp**. One of the contributions to the net loading will therefore be the aerodynamic load which results from this elastic warp. We may express the total aerodynamic load as the sum of the load due to elastic warp and the load which would act over the aircraft if the deformation were removed, without changing the datum incidence or control deflection**. The configuration on which this latter load would act may be identified with that of a hypothetical rigid aircraft which can

---

*Elastic warp corresponds in the present three-dimensional approach to what was termed 'elastic camber' in the two-dimensional treatment in Ref. 1.

**The terms 'datum incidence' and 'datum control deflection' refer to quantities defined for the aircraft as a whole: 'datum' will be omitted when no confusion with local quantities is likely to arise. Their precise meanings will be considered later (Section 2.3): their immediate intuitive meanings are sufficient at this stage.

serve as a datum for assessing aeroelastic effects. It should be noted that the rigid aircraft thus envisaged will not in general be in steady flight for those combinations of incidence and control deflection that produce such conditions for the actual flexible aircraft.

It is now assumed that the distributed loading may be adequately represented by a number of discrete loads Q_i at a set Σ_1 of n_1 points and we write

$$\{Q_i\}_1 = \{\bar{Q}_i\}_1 + \{\Delta Q_i\}_1 \tag{1}$$

where ΔQ_i is the contribution to Q_i resulting from elastic warp. (*See* list of symbols for explanatory notes on notation).

Further, it is assumed that the structural flexibility is described by a square matrix of flexibility influence coefficients $\mathscr{S}$ which relates the deflections w_i at a set Σ_2 of n_2 points to a set of loads L_i at these same points by

$$\{w_i\}_2 = \mathscr{S}\{L_i\}_2 . \tag{2}$$

To find the deflections w_i due to the loads Q_i, in the general case where Σ_1 and Σ_2 do not coincide, we transform the vector $\{Q_i\}_1$ to an equivalent vector $\{L_i\}_2$, expressing the transformation through a matrix $\mathscr{E}$:

$$\{L_i\}_2 = \mathscr{E}\{Q_i\}_1 . \tag{3}$$

Hence

$$\{w_i\}_2 = \mathscr{S}\mathscr{E}\{Q_i\}_1 . \tag{4}$$

We now turn to the calculation of $\{\Delta Q_i\}_1$ corresponding to the deflections $\{w_i\}_2$. Assume that an aerodynamic influence matrix $\mathscr{R}$ can be determined of which the general element $\mathscr{R}_{jk}$ (load/radian) represents the increment in load at a general point j of a set Σ_3 of n_3 points due to an increment in local incidence at a general point k of a set Σ_4 of n_4 points. Denoting the vectors of loads in Σ_3 and incidences in Σ_4 by $\{P_i\}_3$ and $\{\alpha_i\}_4$ respectively, we have

$$\{P_i\}_3 = \mathscr{R}\{\alpha_i\}_4 . \tag{5}$$

Suppose that elastic incidences α_i are determined from the deflections w_i through the relationship

$$\{\alpha_i\}_4 = \mathscr{C}\{w_i\}_2 . \tag{6}$$

Then the aerodynamic loading due to distortion is represented by a set of loads P_i in Σ_3 given by

$$\{P_i\}_3 = \mathscr{R}\mathscr{C}\mathscr{S}\mathscr{E}\{Q_i\}_1 . \tag{7}$$

Finally, $\{\Delta Q_i\}_1$ is determined by replacing the loads P_i in Σ_3 by an equivalent set of loads ΔQ_i in Σ_1, the relationship between them being expressed by a matrix $\mathscr{F}$:

$$\{\Delta Q_i\}_1 = \mathscr{F}\{P_i\}_3 . \tag{8}$$

Hence

$$\{\Delta Q_i\}_1 = \mathscr{F}\mathscr{R}\mathscr{C}\mathscr{S}\mathscr{E}\{Q_i\}_1 \tag{9}$$

$$= \mathscr{L}\{Q_i\}_1 , \text{ say} . \tag{10}$$

We now have from equation (1)

$$\{\Delta Q_i\}_1 = \{Q_i\}_1 - \{\bar{Q}_i\}_1 = \mathscr{L}\{Q_i\}_1 \tag{11}$$

or

$$\{Q_i\}_1 = [\mathscr{I} - \mathscr{L}]^{-1}\{\bar{Q}_i\}_1 \tag{12}$$

If, then, we have a discrete load approximation (the loads $\bar{Q}_i$) to the continuous loading on a hypothetical rigid aircraft we may determine the corresponding approximation (the loads Q_i) for the flexible aircraft through the application of equation (12). For this purpose it is necessary, in the most general case, to determine

(i) a structural flexibility influence matrix $\mathscr{S}$ associated with a set of points Σ_2,

(ii) a matrix $\mathscr{E}$ which transforms a vector of loads in Σ_1 to an equivalent vector of loads in Σ_2,

(iii) an aerodynamic influence matrix $\mathscr{R}$ which gives the aerodynamic loads in Σ_3 corresponding to local elastic incidences in Σ_4,

(iv) a matrix $\mathscr{C}$ which transforms deflections in Σ_2 to local elastic incidences in Σ_4,

(v) a matrix $\mathscr{F}$ which transforms a vector of loads in Σ_3 to an equivalent vector of loads in Σ_1.

The above analysis applies only if $[\mathscr{I} - \mathscr{L}]$ is not singular. Since $\mathscr{L}$ depends on kinetic pressure there may exist airspeeds for which $[\mathscr{I} - \mathscr{L}]$ becomes singular corresponding to the physical phenomenon of static aeroelastic divergence. In principle these divergence speeds could therefore be found by determining the conditions for $[\mathscr{I} - \mathscr{L}]$ to become singular; in practice, however, the numerical processes involved would become unreliable as such conditions were approached. Further discussion of such difficulties will not be attempted here and we shall assume that all cases to be investigated are sufficiently far from cases of divergence for the inversion of $[\mathscr{I} - \mathscr{L}]$ to be a well-conditioned process.

2.3. *The Theory in a Practical Form.*

The above sketch of the theory has presented the idea behind the method. The purpose of this Section is to consider some of the practical difficulties which must be resolved before it can be applied, while still retaining considerable generality.

For a particular quasi-steady flight condition the loading system $\{\bar{Q}_i\}_1$ can be compounded from the known mass distribution and the component aerodynamic loads (derived from calculations and/or wind tunnel tests for the rigid aircraft) provided that the appropriate incidence and control deflection have been specified. These are, however, not known in advance and have in fact to be determined from considerations of the overall equilibrium of the *flexible* aircraft. Indeed, the interpretations to be placed upon the terms 'incidence' and 'control deflection' for the flexible aircraft are not yet defined since no particular system of axes has been assumed.

A question arises in connection with the specification of the structural influence matrix $\mathscr{S}$. Influence coefficients are normally evaluated experimentally or theoretically for the aircraft subjected to a statically determinate system of constraints and it is not immediately apparent whether or not a matrix of coefficients so obtained can be directly applied in the determination of the deformation of a freely flying aircraft. It will transpire that, for the method here developed, we may proceed on the assumption that $\mathscr{S}$ relates to the aircraft constrained in any convenient statically determinate manner. The deflections so obtained will be referred to a certain datum, the selection of which depends on the chosen constraints. For symmetric load systems it is most natural to apply the constraints at points along the centreline of the aircraft. One possibility is to assume that the aircraft is 'simply supported' at two points (at each of which a force but no moment may be applied), another to assume that the aircraft is 'built in' at a single point. In the former situation a suitable datum from which to measure the deflections (and the elastic incidences) is the plane, perpendicular to the plane of symmetry, which contains the two support points, while in

the latter situation a suitable datum plane is tangential to the line of material particles adjacent to the point where the aircraft is 'built in'.

When the datum plane for measuring deflections has been decided upon, the basis for defining 'incidence' is fixed. This is defined as the angle of the datum plane to the free stream (or an angle differing from it by a constant amount). Here we define 'control deflection' simply by identifying it with the deflection of the control surface when the elastic deformation is removed, that is with the control deflection for the hypothetical rigid aircraft. This is convenient for our present purposes, whatever might be its shortcomings as a general definition for a flexible aircraft.

We now turn to the problem of the determination of $\{\bar{Q}_i\}_1$. In any particular case $\{\bar{Q}_i\}_1$ will be compounded from a number of loading systems; aerodynamic, inertial and gravitational. Let a typical unit component system be $\{\bar{Q}_i\}_1^r$ and its contribution to $\{\bar{Q}_i\}_1$ be determined by factoring it by a_r; i.e.

$$\{\bar{Q}_i\}_1 = \sum_r a_r \{\bar{Q}_i\}_1^r \tag{13}$$

and

$$\{Q_i\}_1 = \sum_r a_r \{Q_i\}_1^r \tag{14}$$

where

$$\{Q_i\}_1^r = [\mathscr{I} - \mathscr{S}]^{-1} \{\bar{Q}_i\}_1^r . \tag{15}$$

Two problems remain:

(i) The validity of using the structural influence matrix $\mathscr{S}$ appropriate to the constrained aircraft has still to be established.

(ii) A method of determining the factors a_r has to be found. (For a particular flight condition all of these are known except the two which define the datum incidence and control deflection.)

These problems may be resolved by the following method. Assume that the incidence is defined in a way compatible with the constraints used in the determination of $\mathscr{S}$. Then the load on the free-flying aircraft may be found by determining the aeroelastically modified loading system $\{Q_i\}_1^r$ corresponding to each system $\{\bar{Q}_i\}_1^r$, with the aircraft constrained, and then combining these modified systems according to equation (14), for which the unknown factors a_r are found by applying the conditions of overall equilibrium of the aircraft. Since the resulting $\{Q_i\}_1$ is a self-equilibrating system, the aggregate of the constraining loads corresponding to the component loadings $a_r \{Q_i\}_1^r$ must also form a self-equilibrating system and, since a statically determinate system of constraints has been assumed, it follows that each of the resultant constraining loads must be zero. $\{Q_i\}_1$ is thus appropriate to the free-flying condition.

2.4. *Some Concepts in the Analysis of Aeroelastic Effects.*

The most usual type of investigation into the significance of aeroelasticity proceeds as follows. Suppose that the shape of a certain aircraft, actual or projected, is known when the aircraft is unloaded. This shape will usually be one for which extensive programmes of calculations and wind-tunnel tests have been carried out. Then, if the structural properties of the aircraft are also known, stability and control and loading analyses may be performed:

(a) assuming the aerodynamic shape to remain unchanged from the unloaded condition, apart from control deflections, for all conditions of flight, and

(b) taking full account of structural deformations and the attendant changes in aerodynamic shape and loading.

The differences between the results of (a) and (b) indicate the degree of importance to be attached to

aeroelastic effects in the stability and control and loading analyses for this particular aircraft. We term such differences *gross* aeroelastic effects.

In the aircraft design stage a rather different approach can be used. Suppose that in his attempts to obtain the best possible performance from a design, which can be varied within limits, a designer assumes that it is sufficient to concentrate on the performance at a particular combination of height, speed, weight, etc. This combination we will term the *design point*. When, on the basis of wind-tunnel tests (on nominally rigid models) and calculation, a designer is satisfied with the design-point performance he may be loath to risk any seriously adverse aeroelastic effects on that performance. These may be avoided if the deformations that would occur under the design-point loading are determined and equal but opposite deformations, which we call *compensatory warp*, are built into the aircraft. The aircraft will then assume the required shape, and hence loading, at the design point. It should be noted that the procedure is rather simpler than in most aeroelastic problems in that the deflected shape of the flexible aircraft (with compensatory warp) is known and hence the loading may be found directly: the compensatory warp then follows from a purely structural analysis. Stability and control and loading analyses may now be performed:

(c) for a hypothetical rigid aircraft having the shape required at the design point (identical to (a) above), and

(d) for the actual flexible aircraft built with compensatory warp.

The differences between (c) and (d) represent the residual aeroelastic effects that remain after those associated with the deformations which would occur under the design-point loading have been nullified by the incorporation of compensatory warp. These we term *net* aeroelastic effects.

By definition the net effects on trim conditions are zero at the design point and in most cases they are likely to be smaller than the corresponding gross effects although in certain circumstances they can be greater. For those quantities which depend not on a particular initial condition but on the behaviour when passing from one steady condition to a neighbouring one at constant speed and Mach number, such as the elevator deflection per g, net and gross effects are equal. For those quantities which relate to changes of speed and/or Mach number, such as the slope of the curve of elevator deflection to trim, net and gross effects are in general not equal: the former are, however, not zero even when the initial condition is the design point.

Both gross and net effects are significant to the designer. The order of magnitude of the former should be determined at a fairly early design stage so that the importance of allowing for aeroelastic effects can be assessed. This assessment could indicate that, while in certain flight conditions the effects of aircraft flexibility should be taken into account, such effects would be so small at the design point as to render the incorporation of compensatory warp unnecessary. In such circumstances the aircraft would be built to the original design shape and the concept of net aeroelastic effects would be irrelevant. However, when compensatory warp is incorporated it is still necessary to know what are the net effects.

It seems desirable that in any aeroelastic investigation one should consider both gross and net effects although it will usually be unnecessary to cover both in equal detail. Gross effects should probably be given greater emphasis since they relate to the somewhat more fundamental concept.

2.5. *Method of Calculation for an Aircraft with Built-in Compensatory Warp.*

The previous section considered the possibility of employing built-in compensatory warp to nullify aeroelastic effects at a design condition, and introduced the concept of net aeroelastic effects. We now consider how the method of this Report can allow us to compute such net effects.

Suppose that the loading at the design point is represented by a vector $\{Q_i^D\}_1$. Then the required compensatory warp is given by deflections w_i^D where

$$\{w_i^D\}_2 = -\mathscr{S}\mathscr{E}\{Q_i^D\}_1 . \tag{16}$$

At any other flight condition, where the net load on the aircraft is $\{Q_i\}_1$, the deflections of the aircraft with compensatory warp, relative to the 'design' shape, are

$$\{w_i\}_2 = \mathscr{S}\mathscr{E}\{Q_i - Q_i^D\}_1 . \tag{17}$$

Hence, the load due to the divergence from the design shape, which arises from the difference between the design-point loading and the loading at any other flight condition, is given by

$$\{\Delta Q_i\}_1 = \mathscr{F}\mathscr{R}\mathscr{C}\mathscr{S}\mathscr{E}\{Q_i - Q_i^D\}_1 = \mathscr{L}\{Q_i - Q_i^D\}_1 . \tag{18}$$

Therefore

$$\{Q_i\}_1 - \{\bar{Q}_i\}_1 = \mathscr{L}\{Q_i - Q_i^D\}_1 \tag{19}$$

or

$$\{Q_i\}_1 = [\mathscr{I} - \mathscr{L}]^{-1}\{\bar{Q}_i\}_1 - [\mathscr{I} - \mathscr{L}]^{-1}\mathscr{L}\{Q_i^D\}_1 . \tag{20}$$

It is seen that the above equation is identical with equation (12) save for the addition of a term on the right hand side. The vector $-\mathscr{L}\{Q_i^D\}_1$ must be calculated and premultiplied by $[\mathscr{I} - \mathscr{L}]^{-1}$ in the same way as the load vectors $\{\bar{Q}_i\}_1^r$. The resulting vector is then simply combined with the vectors $\{Q_i\}_1^r$ subject to the conditions of overall equilibrium.

Equation (20) may be looked at from two points of view. The first is that which was adopted in its development; that the deflections are measured relative to the shape of the hypothetical rigid aircraft (without compensatory warp) and that the additional term arises purely from the incorporation of the compensatory warp in these deflections, in accordance with equation (17). A second point of view is that the 'datum' shape is the unloaded shape of the flexible aircraft *with* compensatory warp. Then to the set of load vectors must be added one giving the aerodynamic load due to the difference between this datum shape and the shape of the hypothetical rigid aircraft. If this load vector is calculated through the same aerodynamic matrix as is employed to calculate the aeroelastic deflections it becomes $-\mathscr{L}\{Q_i^D\}_1$. The additional term in equation (20) is then the aeroelastically modified form of this extra load vector.

The second of these points of view is useful in providing us with terminology: we speak of the additional vector $-\mathscr{L}\{Q_i^D\}_1$ as the 'load due to compensatory warp'. The first point of view is perhaps the better one for analytical discussions as it makes clear the fact that the method used to calculate loads due to aeroelastic distortion has to be sufficiently accurate only for loads due to deflections $(w_i - w_i^D)$, which will usually be smaller than deflections w_i. Calculations of net aeroelastic effects should therefore be rather more reliable than those of gross effects, at least for those trimmed level-flight conditions where the overall loading resembles the design-point loading. An additional indication is that it will normally be unprofitable to use a method to calculate the load due to compensatory warp which differs from that applied to aeroelastic distortion, as could justifiably be done in accordance with our complete freedom in determining individual load systems, so replacing the term $-\mathscr{L}\{Q_i^D\}_1$ by some other vector. (The use of a different method would mean that the design-point conditions would not be exactly satisfied, but this would be of no practical significance.)

3. *An Example of the Application of the Method.*

The above method has been used to determine the static aeroelastic effects on a slender aircraft in symmetric flight at a Mach number of 2·2. The general arrangement of the aircraft, which is an early projected version of the Anglo-French 'Concorde' airliner, is shown in Fig. 1. The weights and kinetic pressures assumed for the start, middle and end of cruise are appropriate to the medium range version.

The structural flexibility matrix and the data from which were derived the inertial and (untrimmed) aerodynamic loadings for the rigid aircraft were provided by the British Aircraft Corporation (Operating) Ltd., Filton Division. The sizes of the matrices which could be employed were initially dictated by limita-

tions of computer capacity, on the assumption that the calculations would be performed on the R.A.E. 'Mercury' computer. In the event, 'Mercury' failed inexplicably to perform certain operations programmed for it and some of the work had to be performed on the 'Atlas' computer at Manchester. Had the use of this computer been envisaged at the outset, larger matrices could have been employed with (presumably) beneficial effects on accuracy.

The British system of units is that basically employed. When certain numerical values first appear in the text their equivalents in SI units are given in parentheses. Values in SI units are indicated on the illustrations by means of auxiliary scales.

Since this is a symmetric problem we need consider directly only the loads acting on either the port or the starboard half of the aircraft. We take account of the loads and elastic incidences on the other half by modifying the matrices $\mathscr{S}$ and $\mathscr{R}$. (The starboard half was actually chosen.)

3.1. *The Matrices Employed.*

3.1.1. $\mathscr{S}$, *the structural flexibility influence matrix.* Three such matrices were made available by the British Aircraft Corporation. These were associated with sets of 75, 121 and 200 points respectively (per half-wing) and had been obtained in the course of a displacement-type structural analysis. The present investigation was initially limited in the choice of Σ_1 to sets which contained less than 100 points and so, following the considerations in Appendix A, the matrix associated with 75 points was chosen. The set of structural grid points is shown in Fig. 2. The 'half-aircraft' is constrained by two simple supports. These do not lie on the centreline; however, as the problem is symmetric, the implied complete constraint system of four simple supports is still statically determinate.

The matrix $\mathscr{S}$ took account of the fact that for every load at a grid point on the starboard half of the aircraft there is an equal load at the corresponding point on the port half, which causes additional deflections on the starboard half.

It is seen that the grid points give good coverage of most of the half-aircraft; the main regions which are omitted are (i) the fuselage inboard of a line near the wing root, (ii) the elevators, (iii) the portion of the wing to the rear of (approximately) the elevator hinge line, and (iv) the portion of the fuselage to the rear of the aft support point. The assumptions which were made to allow for these omissions are:

(i) the fuselage is rigid in a spanwise direction,

(ii), (iii) to the rear of the last row of grid points there is no change in elastic incidence along any chordwise line, and

(iv) the fuselage load to the rear of the aft support point causes no deflections.

Of these the last is probably the most questionable but the choice of Σ_2 and the method of deriving the component load systems made it necessary – it is thought to lead to only small errors.

3.1.2. $\mathscr{E}$, *the load vector transformation matrix between* Σ_1 *and* Σ_2. The twin considerations of computer capacity and the need to ensure that, over the region of action of any component loading, Σ_1 gives a coverage at least as dense as Σ_2 gave close limits for the number of points in Σ_1. Accordingly it was decided to choose Σ_1 to coincide with Σ_2. Hence the matrix $\mathscr{E}$ becomes the unit matrix and may be omitted from the equations.

3.1.3. $\mathscr{R}$, *the aerodynamic influence matrix.* A matrix of aerodynamic influence coefficients based on steady, linearised, supersonic-flow theory was required. The method described by Lees[2] offered a direct approach to the calculation of such influence coefficients, and this method was accordingly adopted. For its application the wing is subdivided into diamond-shaped panels by a network of equispaced Mach lines, and the velocity potential induced at each receiving panel by unit downwash at every other panel in turn is calculated. The corresponding lift per unit downwash is obtained by integrating the potential over the edges of the receiving panel. Only panels lying within the forward Mach cone from the aftmost corner of a given panel can contribute to the lift at that panel and when, as in the present example, the leading edges of the wing are subsonic, the precise area within which 'effective' panels lie is defined by application of Evvard's area cancellation technique. The influence of the jth panel on the ith panel depends only on parameters m, n defining the *relative* positions of the two panels in a system

of oblique axes parallel to the Mach lines*. In his paper, Lees has tabulated the relevant influence function $A(m,n)$ for values of m and n over the ranges $1 \leqslant m \leqslant 11$, $1 \leqslant n \leqslant 21$, and this provides the basis for a straightforward, if somewhat tedious, compilation of the influence coefficient matrix for the complete wing. The matrix thus obtained actually gives loads per unit kinetic pressure – we denote it by $\mathscr{R}^*$. $\mathscr{R}$ is obtained by multiplying $\mathscr{R}^*$ by Q.

In the present application the method was applied to the complete aircraft planform, excluding the portion of the fuselage extending behind the wing trailing edge. Advantage was again taken of the symmetrical nature of the problem so that Σ_3 and Σ_4 (which in this case coincide) were defined over the starboard half of the aircraft only. Mesh size was fixed by taking the length of the longer diagonal of a panel to be 1/11 of the overall length of the assumed planform. The resulting mesh divided the half-aircraft into 60 panels of diamond or partial diamond shape as shown in Fig. 2. For clarity the mesh is shown on the port half. The points of Σ_3 and Σ_4 are located at the centroids of panels. For each panel l on the starboard half-wing we may envisage a symmetrically disposed panel l' on the port half-wing. The element $\mathscr{R}_{lk}$ of $\mathscr{R}$ then represents the point load at grid point k due to unit incidence of the pair of panels l, l'.

With this size of mesh, the influence coefficients could be calculated directly from Lees's tabulated values of $A(m,n)$. Although the number of points in the Σ_3 thereby obtained is lower than the number in Σ_1, the 'densities' of the two sets of points are comparable over most of the aircraft. Hence there is no serious violation of the requirement (Appendix A) that the density of Σ_3 be at least as high as that of Σ_1.

As was noted earlier, assessment of accuracy was not one of the aims of the present investigation. However, for interest's sake, the load per radian incidence of the rigid aircraft as predicted by $\mathscr{R}$ was compared with that which was used as a basis for the loading component $\{\bar{Q}_i\}_1^a$ (*see* Section 3.2.3). The lift-curve slope which was obtained was 2·23 whereas a value of 2·0 was assumed for $\{\bar{Q}_i\}_1^a$. The aerodynamic centre was given at $0{\cdot}559c_0$ by $\mathscr{R}$ and at $0{\cdot}592c_0$ by $\{\bar{Q}_i\}_1^a$. Examination of the two lengthwise loadings shows that most of the discrepancy in the position of the aerodynamic centre is due to the fact that the use of $\mathscr{R}$ leads to overestimation of the loading on the forward part of the fuselage. Further refinement was not thought worthwhile at this stage.

3.1.4. *The matrices $\mathscr{C}$ and $\mathscr{F}$.* It will be recalled that, in the general theory, $\mathscr{C}$ is the matrix which transforms deflections at the set Σ_2 of structural grid points into local elastic incidences at the set Σ_4 of downwash points associated with $\mathscr{R}$, while matrix $\mathscr{F}$ transforms a vector of loads in Σ_3 to an equivalent vector of loads in Σ_1. As already noted, in the present application, $\Sigma_1 \equiv \Sigma_2$ and $\Sigma_3 \equiv \Sigma_4$, so that in effect $\mathscr{C}$ transforms deflections at the structural grid points into local incidences at the aerodynamic grid points and $\mathscr{F}$ transforms a vector of loads at the aerodynamic grid points into an equivalent vector of loads at the structural grid points.

Basically, the methods adopted for the calculation of elements of these matrices were those suggested by Williams[3]. Some extensions were necessary in order to deal with certain regions of the planform (notably the fuselage and elevon portions) where the ideas of Williams are not directly applicable.

3.2. *The Component Loadings.*

For this investigation all the component loadings were taken to act over the same set of points Σ_1 although, as discussed in Appendix A, this need not generally be the case. The following rigid aircraft component loadings were considered.

$\{\bar{Q}_i\}_1^I$ Inertial load (per g) for the aircraft with zero fuel.

$\{\bar{Q}_i\}_1^F$ Inertial load (per g) due to fuel.

$\{\bar{Q}_i\}_1^C$ Aerodynamic load for a C_L of 0·1.

---

*If Q is the aftmost corner of panel i, and P is the foremost corner of panel j, the oblique co-ordinates of P relative to Q are ml and nl where l is the length of the panel side.

$\{\bar{Q}_i\}_1^{\alpha}$ Aerodynamic load due to incidence.

$\{\bar{Q}_i\}_1^{\eta}$ Aerodynamic load due to elevator deflection.

$\{\bar{Q}_i\}_1^{q}$ Aerodynamic load due to rate of pitch.

We now discuss the formation of each of the above loading vectors. For the aerodynamic components the so-called load vectors are in fact to be interpreted as vectors of loads divided by the free stream kinetic pressure.

In addition to these vectors, the vector $-\mathscr{F}\mathscr{R}^*\mathscr{C}\mathscr{S}\{Q_i^D\}_1$, giving the load due to compensatory warp, was computed. We denote this by $\{\bar{Q}_i\}_1^W$. The design point is defined in Section 3.5.

3.2.1. *Inertial loading for the aircraft with zero fuel.* The distribution of mass for the aircraft with zero fuel was supplied by the British Aircraft Corporation in the form of discrete loads at the nodal points of the 200-point structural grid. These were re-distributed to the nodes of the 75-point grid. The loads at points of the 200-point grid lying within the wing planform aft of the elevon hinge line were transferred forward to the rearmost grid line of the 75-point grid (approximately coincident with the elevon hinge line) and then shared in appropriate proportions between the nearest grid points on either hand. Transfer moments about the grid line in question were considered to have no effect on deflections at points of the 75-point grid, but were preserved for inclusion in the equations of overall equilibrium for the aircraft. Similarly, loads at points on the rearbody aft of the rearmost grid line were neglected as regards their effect on deflections at points of the 75-point grid, but were accounted for in the equations of overall equilibrium.

3.2.2. *Inertial loading due to fuel.* As shown in Fig. 3, the aircraft has six fuel tanks per side and a single tank in the tail cone. The mass of fuel contained in each tank when full is given below (that for the tail tank being per side).

Tank No.	1	2	3	4	5	6	7
Mass of fuel, lb	5080	9790	7110	14133	12870	7050	6615
(kg)	(2304)	(4441)	(3225)	(6411)	(5838)	(3198)	(3000)

The inertial loading for each tank when full was derived in the same way as the inertial loading for the aircraft with zero fuel. Let the load vector corresponding to the rth tank be $\{\bar{Q}_i\}_1^{Fr}$. Then we express the inertial loading due to a particular fuel loading as

$$\{\bar{Q}_i\}_1^F = \sum_{r=1}^{6} k_r \{\bar{Q}_i\}_1^{Fr}. \qquad (0 \leqslant k_r \leqslant 1) \tag{21}$$

Note that there is no vector corresponding to the fuel in the tail tank, by virtue of assumption (iv) in Section 3.1.1: the force and moment due to this fuel were included in the conditions of overall equilibrium.

3.2.3. *Aerodynamic loading for the aircraft with undeflected controls and zero rate of pitch (components* $\{\bar{Q}_i\}_1^C$ *and* $\{\bar{Q}_i\}_1^{\alpha}$). Aerodynamic loading data for the rigid aircraft at $M = 2{\cdot}2$ were made available by British Aircraft Corporation in the form of:

(1) Longitudinal load distribution curves ($L(x)$: load per unit length per unit kinetic pressure, *versus* x: distance from nose of aircraft) for values of the untrimmed lift coefficient C_L from $-0{\cdot}1$ to $0{\cdot}4$ in steps of $0{\cdot}1$.

(2) Spanwise load distribution curves (local loading coefficient *versus* fraction of local semispan from centreline) for eight chordwise stations at the same C_L values as for (1).

This information was based partly on wind-tunnel tests and partly on theory. As already indicated in Section 3.2, it was decided to express the aerodynamic loading for the aircraft with undeflected controls and zero rate of pitch as the sum of two components; one corresponding to an arbitrarily chosen C_L of 0·1 (corresponding roughly to the design point) and the other to the incremental incidence relative to the $C_L = 0{\cdot}1$ value. The starting points for the derivation of the loading vectors $\{\bar{Q}_i\}_1^C$ and $\{\bar{Q}_i\}_1^\alpha$ were therefore the $L(x)$ *versus* x curve for $C_L = 0{\cdot}1$, taken directly from the B.A.C. data, and a curve of incremental loading $\Delta L(x)$, per radian of incidence, *versus* x, deduced from the set of $L(x)$ *versus* x curves, under the assumption that $\frac{dC_L}{d\alpha} = 2{\cdot}0$ over the range $-0{\cdot}1 < C_L < 0{\cdot}4$. The two basic loading curves $[L(x)]_{C_L = 0{\cdot}1}$ and $\frac{\Delta L(x)}{\Delta\alpha}$ *versus* x are shown in Fig. 4. To convert these distributed loadings to the equivalent discrete load vectors $\{\bar{Q}_i\}_1^C$ and $\{\bar{Q}_i\}_1^\alpha$, the total load in each case had first to be apportioned to chordwise stations corresponding to spanwise grid lines of the structural grid; the load at each chordwise station had then to be distributed to the grid points at that station in a manner consistent with the spanwise load distribution curves supplied by B.A.C. Graphical interpolation was used to derive from these curves the spanwise distribution curves appropriate to the chordwise stations of the structural grid.

In the apportionment of load to chordwise stations the general principle adopted was to assume the longitudinal distribution between two adjacent stations to be trapezoidal and to replace it by a pair of concentrated loads at those stations, which gave the same total load and c.p. position. Thus, in general, the load allocated to a particular chordwise station comprised two contributions, derived from the continuous load distributions in the two intervals between that station and its immediate neighbours. The loading ahead of the foremost structural grid point, G.P.75, was replaced by concentrated loads at G.P.'s 74 and 75 to give the same total load and c.p. position, while the loading aft of the elevon hinge line was assumed to be concentrated along the rearmost structural grid line, an appropriate transfer moment being computed for inclusion in the overall balance equations.

In general, for a given chordwise station, the (spanwise) distribution of the total load between the structural grid points at that station was determined in a manner analogous to that adopted for the chordwise allocation. In order to derive the point loads corresponding to the distributed load inboard of the first row of grid points a row of 'dummy' points along the centreline was introduced. This done, the procedure was perfectly straightforward for stations with a full complement of grid points; where, however, a spanwise row of points was incomplete (*see* Fig. 2), further 'dummy' grid points were introduced to complete the set, and the load was first distributed between this complete set of actual and 'dummy' grid points. The load at each 'dummy' point was subsequently replaced by a statically equivalent pair of loads at the nearest two actual grid points on the same chordwise grid line. At stations on the forward part of the wing where there were only two or three grid points, 'dummy' points were introduced at locations chosen so as to ensure that the continuous spanwise distribution was broken down into approximately trapezoidal portions. In this case, the load at each 'dummy' point was replaced by a statically equivalent pair of loads at the nearest two actual grid points on the spanwise grid line under consideration. Loads at the aircraft centreline were transferred directly outboard to the first chordwise row of grid points. The resultant of the continuous loading outboard of the last grid point on a spanwise grid line was estimated separately and replaced by a pair of loads at the nearest two grid points.

A digital computer ('Mercury') program was prepared to perform the initial allocation of load to the grid points (actual and 'dummy') of the various chordwise stations. Subsequent manipulation of the loads was performed by hand.

3.2.4. *Aerodynamic load per radian elevator deflection.* The aircraft has three trailing edge control surfaces (elevons) per side, as shown in Fig. 3. It was assumed that any of these could be used for pitch control (i.e. as elevators) and that the ratios of the deflections of the individual surfaces could take any non-negative values. Accordingly, the deflection of any surface, say the rth, may be expressed as $g_r\eta$, where η is the largest of the three control surface deflections and is termed the 'control (elevator) deflection'.

Therefore if the load vector corresponding to unit deflection of the rth control surface is $\{\bar{Q}_i\}_1^r$ the total load vector per unit elevator deflection is

$$\{\bar{Q}_i\}_1^\eta = \sum_{r=1}^{3} g_r \{\bar{Q}_i\}_1^r . \tag{22}$$

The loadings were calculated by linear supersonic theory[6]. The load vectors were derived by transferring the load on the control surfaces to the rearmost line of grid points, while preserving the spanwise positions of the centres of pressure (no load was transferred to the grid point nearest the tip). Again, the correct balance was preserved by the addition of transfer moments in the equations of overall equilibrium.

3.2.5. *Aerodynamic load due to rate of pitch.* No wind-tunnel data exist on the aerodynamic load due to rate of pitch. This loading was therefore calculated using the aerodynamic influence matrix. (For the present example of a slender aircraft at high speed its effect will be small but it was included for the sake of completeness.) Consider first the loading to act in Σ_3. Let a typical point of Σ_4 and the centre of gravity of the aircraft be distances x_i' and $\bar{x}$ ahead of an arbitrary fixed point (here taken as the aft support point). Then the incidence induced at this typical point by a rate of pitch q about the centre of gravity is

$$-(x_i'-\bar{x})\, q/V . \tag{23}$$

Thus the load vector in Σ_3 due to unit rate of pitch is

$$\{\bar{P}_i\}_3^q = -\frac{1}{V}\mathscr{R}^* \{x_i'\}_4 + \frac{\bar{x}}{V}\mathscr{R}^* \{\mathscr{I}_i\}_4 , \tag{24}$$

where $\{\mathscr{I}_i\}_4$ is a unit column.

Now $q = (n-1)\, g/V$, where ng is the total normal acceleration†, and since V is constant over the range of kinetic pressure (or altitude) being considered, we may express the above loading as a loading due to incremental normal acceleration. Hence, in Σ_1, the loading due to rate of pitch can be expressed as

$$(n-1)\{\bar{Q}_i\}_1^q = (n-1)\{\bar{Q}_i\}_1^{q1} + \bar{x}\,(n-1)\{\bar{Q}_i\}_1^{q2} \tag{25}$$

where

$$\{\bar{Q}_i\}_1^{q1} = -\mathscr{F}\mathscr{R}^*\{x_i'\, g/V^2\}_4 \tag{26}$$

$$\{\bar{Q}_i\}_1^{q2} = \mathscr{F}\mathscr{R}^*\{\mathscr{I}_i\, g/V^2\}_4 . \tag{27}$$

3.3. *The Conditions of Overall Equilibrium.*

The conditions of overall equilibrium for the aircraft in quasi-steady flight with a normal acceleration of ng were satisfied by equilibrating the forces normal to the datum plane and the moments about the rearmost line of structural grid points.

Let the force and moment corresponding to the load vector $\{Q_i\}_1^I$, for example, be Z_I and M_I respectively. Included in such forces and moments are any additional forces and moments not accounted for in the load vectors (*see* for example Section 3.2.1). Then the equilibrium equations are

† Note that in Ref. 1 the total normal acceleration was denoted by $\bar{n}g$, ng being there the incremental normal acceleration from level flight. This revision is in accordance with the usual practice when discussing structural loading.

$$Q\{Z_C+\alpha Z_\alpha+\eta Z_\eta+(n-1) Z_q+Z_W\}+n(Z_I+Z_F)=0 \tag{28}$$

and

$$Q\{M_C+\alpha M_\alpha+\eta M_\eta+(n-1) M_q+M_W\}+n(M_I+M_F)=0\,, \tag{29}$$

where

$$Z_F=\sum_{r=1}^{7} k_r Z_{Fr} \tag{30.1}$$

$$M_F=\sum_{r=1}^{7} k_r M_{Fr} \tag{30.2}$$

$$Z_\eta=\sum_{r=1}^{3} g_r Z_{\eta r} \tag{30.3}$$

$$M_\eta=\sum_{r=1}^{3} g_r M_{\eta r} \tag{30.4}$$

(Z_{F7}, M_{F7} and k_7 relate to the fuel in the tail tank).

These equations may be solved for α and η. The chosen method of presentation of results separates out the values of α and η for trimmed level flight (here taken as $n = 1$), α_t and η_t, and the rates of variation of α and η with normal load factor, $d\alpha/dn$ and $d\eta/dn$. Therefore we replace equations (28) and (29) above by two sets of equations:

$$\alpha_t Z_\alpha+\eta_t Z_\eta=-\frac{1}{Q}(Z_I+Z_F)-Z_C-Z_W \tag{31}$$

$$\alpha_t M_\alpha+\eta_t M_\eta=-\frac{1}{Q}(M_I+M_F)-M_C-M_W \tag{32}$$

and

$$\frac{d\alpha}{dn} Z_\alpha+\frac{d\eta}{dn} Z_\eta=-\frac{1}{Q}(Z_I+Z_F)-Z_q \tag{33}$$

$$\frac{d\alpha}{dn} M_\alpha+\frac{d\eta}{dn} M_\eta=-\frac{1}{Q}(M_I+M_F)-M_q\,. \tag{34}$$

The above derivation of the conditions of overall equilibrium is strictly applicable to the flexible aircraft with built-in compensatory warp. For the rigid aircraft the forces and moments become $\bar{Z}_I$ and $\bar{M}_I$, for example, and in this case, and in the case of the flexible aircraft without compensatory warp, Z_W and M_W are omitted.

3.4. *The Resultant Load on the Aircraft.*

When the equilibrium equations have been solved for α_r, η_t, $d\alpha/dn$ and $d\eta/dn$ the resultant load on the aircraft may be found. The point loads Q_i are given by

$$\{Q_i\}_1 = n\{Q_i\}_1^I + n\{Q_i\}_1^F + Q\left[\{Q_i\}_1^C + \alpha_t\{Q_i\}_1^\alpha + \eta_t\{Q_i\}_1^\eta + \{Q_i\}_1^W\right]$$

$$+ Q(n-1)\left[\frac{d\alpha}{dn}\{Q_i\}_1^\alpha + \frac{d\eta}{dn}\{Q_i\}_1^\eta + \{Q_i\}_1^q\right].$$

The modifications necessary to make this equation applicable to either the rigid aircraft or the flexible aircraft without compensatory warp are obvious.

3.5. *Definition of the Design Point and other 'Standard' Conditions.*

The design point was assumed for the purposes of this example to be a condition in approximately mid-cruise: $M = 2{\cdot}2$ at about 58 000 ft (17 700m). The weight assumed was consistent with data supplied by B.A.C. The distribution of fuel was chosen to be in accordance with a feasible plan of fuel usage during a complete flight and to be such that the rigid aircraft would be trimmed with virtually zero elevator deflection (0·01°).

In addition to the design point, two other 'standard' conditions were defined. These corresponded to points at approximately the start and the end of cruise. The kinetic pressures and weights were again in accordance with B.A.C.'s data while the fuel distribution was chosen to give small elevator angles to trim and to bear a sensible relationship to the design-point distribution.

The detailed specifications of these conditions are

	W lb (kg)	Q lb/ft^2 (kN/m^2)	k_1	k_2	k_3	k_4	k_5	k_6	k_7
Start of cruise	190 330 (86 330)	670 (32·08)	0	0·35	0	1·0	0·54	0·6	0·36
Design point	170 840 (77 490)	550 (26·33)	0	0·35	0	0·62	0·2	0·6	0·36
End of cruise	150 880 (68 440)	450 (21·55)	0	0·2	0	0·2	0	0·6	0·36

3.6. *Results.*

3.6.1. *General scope of calculations performed and results presented.* The calculations were performed for a single Mach number, 2·2, corresponding to the cruise-climb phase of a typical flight plan. This was in the interests of computational economy since the component aerodynamic loadings and the aerodynamic influence matrix $\mathscr{R}^*$ (and its associated transforming matrices $\mathscr{C}$ and $\mathscr{F}$) would have had to have been recalculated for each Mach number considered. With economy again in mind, it was decided to restrict the calculations of trim, manoeuvrability, resultant load distributions and deflections to the three 'standard' weight distributions detailed in Section 3.5. In the practical application of the method to aircraft design it would be necessary to consider a range of Mach numbers, with associated altitudes and weight distributions, corresponding to various points of the flight envelope. Here we have obtained some idea of the effects of operating away from the normal flight plan by making certain calculations for kinetic pressures (and hence altitudes) other than the 'standard' (flight plan) value.

Accordingly, the aeroelastically modified component loading vectors $\{Q_i\}_1'$, detailed in Section 3.2,

were calculated for kinetic pressures of 300, 450, 550, 670, 800 and 1000 lb/ft^2 (14·36, 21·55, 26·33, 32·08, 38·30 and 47·88 kN/m^2), and used in balance calculations for each of the three weight distributions. The altitude corresponding to a particular kinetic pressure may be found from Fig. 5. In all cases three combinations of the control gearings were used, *viz.*

$g_1 = g_2 = g_3 = 1{\cdot}0$: All surfaces moved together.

$g_1 = 0, g_2 = g_3 = 1{\cdot}0$: The inboard surface undeflected, the outboard two moved together.

$g_1 = 1{\cdot}0, g_2 = g_3 = 0$: Only the inboard surface deflected.

The incidences and elevator angles to trim and to sustain steady manoeuvres were determined for each combination of the variations listed above (54 cases in all) and are plotted against kinetic pressure Q in Figs. 6 to 17.

The resultant load distribution was calculated for the three 'standard' flight conditions and also for the design-point fuel distribution at kinetic pressures of 450 and 670 lb/ft^2. In these cases the control gearings were $g_1 = g_2 = g_3 = 1{\cdot}0$. From these load distributions the longitudinal distributions of shear force and bending moment were derived and are presented in Figs. 18 to 32.

The deflections due to elastic warp have been calculated for the design-point flight condition at normal accelerations of 1·0 and 2·5g. For the former the control gearings were $g_1 = g_2 = g_3 = 1{\cdot}0$, while for the latter the three combinations of gearings were considered. These deflections are presented in Figs. 33 to 36. Consideration of these figures (Section 3.6.6) provides some physical explanations of the results of the trim and manoeuvrability calculations.

In the presentation of the trim data and the shear force and bending-moment distributions, three curves are generally distinguishable in each case. These relate respectively to the rigid aircraft, the flexible aircraft and the flexible aircraft with compensatory warp so that, in accordance with the definitions of Section 2.3, the differences between the first and second represent the *gross* aeroelastic effects, while the *net* aeroelastic effects are measured by the differences between the first and third curves. Incremental incidences and elevator deflections for steady manoeuvres are independent of built-in warp so that only two curves appear in the part of each figure presenting these data, and gross and net aeroelastic effects are equal.

3.6.2. *Incidences to trim and incremental incidences per g, α_t and $\frac{d\alpha}{dn}$ (Figs. 6 to 8).* Since for the rigid aircraft the centres of pressure of the three control-surface loadings lie approximately on a spanwise line, the incidences to trim and manoeuvre it are virtually independent (to within 0·01°) of the control gearings here considered. Consequently the 'rigid aircraft' curves in Figs. 6 to 8 can be taken as applying to any of the three combinations of gearings. The effects of aeroelasticity on the required incidences are small. The incidence to trim, α_t, is affected most in the 'start to cruise' fuel configuration with $g_1 = 0, g_2 = g_3 = 1{\cdot}0$, while the greatest effects on $d\alpha/dn$ are in the same fuel configuration but with $g_1 = 1{\cdot}0, g_2 = g_3 = 0$. These effects are shown in Fig. 6. There are similar trends in the other two 'standard' configurations, as shown in Figs. 7 and 8. (As already noted in Section 3.6.1 the incidence and elevator deflections to manoeuvre the flexible aircraft are the same whether or not compensatory warp is included.)

3.6.3. *Elevator deflections to trim, η_t.*

(a) $g_1 = g_2 = g_3 = 1{\cdot}0$ (*Figs. 9 to 11*).

With 'start of cruise' fuel, the gross effect of aeroelasticity is to change η_t by a positive increment, the magnitude of which is reduced by compensatory warp for values of Q below about 800 lb/ft^2 but slightly increased for greater values. With 'design point' fuel, the gross effect of aeroelasticity is again to cause a positive increment in η_t. However, this is small and is only 0·11° at the design point. Therefore the inclusion of compensatory warp purely to avoid a trim drag penalty would not be worthwhile, although other considerations could still lead a designer to incorporate it. In particular, he might wish to ensure that there was no large increase in the drag of the wing itself. The net effect of aeroelasticity on η_t with this fuel distribution is generally smaller than the gross effect, the increment being negative for values

of Q less than the flight plan value (550) and positive for greater values. Aeroelasticity causes a negative increment in η_t with 'end of cruise' fuel, the net effect being greater than the gross except at values of Q very much greater than the flight plan value (450).

(b) $g_1 = 0, g_2 = g_3 = 1{\cdot}0$ (*Figs.* 12 *to* 14).

With this combination of gearings (corresponding to use of the two outboard pairs of controls only) the elevator angles, negative at low Q and positive at high Q, required to trim the rigid aircraft are larger than in case (a). Whereas in that case the gross effect of aeroelasticity was to produce an increment in η_t which was approximately constant throughout the Q range, in the present case the increment increases algebraically with increasing Q. Thus, for example, we see from Fig. 12 that with 'start of cruise' fuel the increment is small and positive for $Q = 300$ but increases such that at $Q = 1000$ the value of η_t for the flexible aircraft is about $1\frac{3}{4}$ times that for the rigid aircraft. A similar trend in the increment in η_t is found for the other two fuel distributions. Differences between gross and net effects of aeroelasticity on η_t are generally small but can be of either sign depending on the particular combination of fuel distribution and kinetic pressure.

(c) $g_1 = 1{\cdot}0, g_2 = g_3 = 0$ (*Figs.* 15 *to* 17).

With these gearings (corresponding to use of inboard controls only) the effects of aeroelasticity on η_t show opposite trends when compared with those in (b). Thus the increment in η_t becomes increasingly negative at high Q whereas in case (b) it became increasingly positive.

3.6.4. *Incremental elevator deflections per g,* $\frac{d\eta}{dn}$. On the 'classical' rigid tailed aircraft, $d\eta/dn$ is proportional to the manoeuvre margin and inversely proportional to the lift curve slope with respect to elevator angle of the tailplane plus elevator. The effects of aeroelasticity are (largely) a change in manoeuvre margin and a change in the power of the elevator to produce lift on the tail. Now, as Taylor has pointed out[1], when calculations which introduce arbitrary constraints are performed for slender flexible aircraft, variations in quantities which correspond to these 'classical' concepts of manoeuvre margin and elevator power do not necessarily have any physical significance. Rather, the behaviour of the unconstrained flexible aircraft has to be considered as a whole. Nevertheless one may still talk in a somewhat loose way about certain effects of aeroelasticity as stemming from a change in one or other of these parameters, by analogy with the 'classical' aircraft, depending on the way in which the aircraft behaves.

In this connection it is worth remarking that in Part 2 of Ref. 1 (Section 4(a)) intuitive reasoning based on these 'classical' concepts was used to predict the variations in elevator effectiveness with elevator location which are discussed in (a) to (c) below.

(a) $g_1 = g_2 = g_3 = 1{\cdot}0$ (*Figs.* 9 *to* 11).

The values of $d\eta/dn$ for the flexible aircraft are lower in absolute value than those for the rigid aircraft for 'start of cruise' fuel but higher for 'design point' and 'end of cruise' fuel. Hence the decrease in manoeuvre margin is dominant for the 'start of cruise' configuration but dominated by the decrease in elevator power in the other two cases. The effects remain largely 'in step' in that the differences between the rigid and flexible aircraft values of $d\eta/dn$ do not vary markedly as Q varies.

(b) $g_1 = 0, g_2 = g_3 = 1{\cdot}0$ (*Figs* 12 *to* 14).

Here, with only the controls on the more flexible outer portion of the wing being deflected, the loss in elevator power is more marked but the difference between the flexible and rigid aircraft values of $d\eta/dn$ still shows no very rapid increase with increasing Q.

(c) $g_1 = 1{\cdot}0, g_2 = g_3 = 0$ (*Figs.* 15 *to* 17).

Since aeroelasticity causes little loss of power for the inboard control the decrease in manoeuvre margin is dominant and the absolute value of $d\eta/dn$ is lower for the flexible aircraft: the difference from the rigid aircraft value decreases somewhat as Q is increased.

3.6.5. *Longitudinal distributions of shear force and bending moment* (*Figs.* 18 *to* 32). It was decided to restrict calculations of load distributions to the cases with control gearings $g_1 = g_2 = g_3 = 1{\cdot}0$. This decision rested on three points:

(i) It was recognised that a reliable reconstruction of the continuous loading was not practicable over the rearmost parts of the aircraft.

(ii) It was assumed that the 'carry-forward' aeroelastic effects on the control-surface loadings would be fairly localised and not greatly affect the loading over most of the aircraft.

(iii) The use of differing control gearings has, as was seen in Section 3.6.2, little effect on the incidences required, even for the flexible aircraft.

From the point loads Q_i it has been possible to derive (approximately) the continuous longitudinal distributions (over the complete aircraft) of shear force $S(x)$ and bending moment $M(x)$. The approximations made in this reconstruction were consistent with the methods used to derive the individual loading vectors. Further, it was assumed that the nose undercarriage could be represented by a point mass of 1150 lb, 56 ft from the nose, and that each main undercarriage could be represented by a point mass of 3750 lb, 109 ft from the nose. $S(x)$ and $M(x)$ are presented, for $n = 1{\cdot}0$, $2{\cdot}5$ and $-0{\cdot}5$, in Figs. 18 to 32. The distributions could not be derived for the foremost parts of the fuselage. Likewise, a region rearward of the last row of grid points in the case of $M(x)$, or a station somewhat ahead of this in the case of $S(x)$, is not covered.

The greatest positive value of $M(x)$ is increased by aeroelasticity, but in the overriding $2{\cdot}5g$ case this increase never exceeds 5 per cent. In the $-0{\cdot}5g$ cases, the considerable negative bending moment which occurs about 130 ft from the nose is little affected. Generally, then, the effects of aeroelasticity on $S(x)$ and $M(x)$ are small. However, one should not assume that more localised loading actions quantities would be as little affected.

3.6.6. *Elastic warp* (*Figs* 33 *to* 36). The elastic warp acquired by the flexible aircraft (without compensatory warp) is shown for a representative set of cases in Figs. 33 to 36. The flight and fuel conditions are those of the design point: the elastic warp is shown for trimmed $1g$ flight, with $g_1 = g_2 = g_3 = 1{\cdot}0$, in Fig. 33 and for $2{\cdot}5g$ flight, with the three combinations of control gearings here considered, in Figs. 34 to 36. The projection of the drawings is isometric, with the deflections being increased in the ratio of 10:1 over distances in the reference plane. The undeflected shape of the aircraft in the reference plane is indicated by dashed lines. In the present case, the deflections of the rearmost parts of the aircraft could not be obtained and the elastic warp can therefore be presented only for the parts forward of the rearmost row of grid points. The chordwise and spanwise variations of the deflections can be judged from the method of presentation adopted for the starboard half of the aircraft, while a more immediate overall impression of the elastic warp can perhaps be obtained from the port half.

In Fig. 33 it is seen that the deflections in $1g$ flight, with $g_1 = g_2 = g_3 = 1{\cdot}0$, are such that the wing undergoes mainly spanwise bending. There is a small amount of wash-out, which leads one to surmise that the elastic warp of the wing produces a positive increment in the value of η_t. This effect is, however, opposed by the effect resulting from the downward deflection of the nose. The forward parts of the aircraft carry a negative increment of lift, which demands a compensating negative increment in η_t. In this case the combined effect of these opposing trends is to produce a small positive increment in η_t ($0{\cdot}11°$).

In Fig. 34 it is seen that when all three controls are used the deflections for a steady $2{\cdot}5g$ manoeuvre result in mainly spanwise bending, though there is a certain amount of wash-out, especially near the tips. Because of the opposing influence of the negative incremental lift on the nose, however, the elevator angle required on the flexible aircraft ($-7{\cdot}47°$) is close to that on the rigid aircraft ($-7{\cdot}30°$).

When only the outer controls are used there is virtually no wash-in or wash-out (Fig. 35). In the absence of incremental lift on the nose, one would expect almost equal elevator angles on the rigid and the flexible aircraft. Therefore the fact that a more negative angle is required on the flexible aircraft, $-14{\cdot}41°$ as against $-11{\cdot}88°$, can probably be attributed largely to the negative incremental lift on the nose.

The use of only the inboard controls results in a mode of deflection consisting of spanwise bending together with considerable wash-out (Fig. 36). In this case the influence of the downward deflected nose

is overcome by the influence of the wash-out on the wing and the elevator angle for the flexible aircraft is $-15{\cdot}56°$, compared with the rigid aircraft value of $-18{\cdot}93°$.

3.6.7. *Comparison with results of other investigations.* The present investigation is by no means the first to seek to determine the effects of aeroelasticity on slender wing aircraft. Of those that have been conducted in the past, that reported in R. & M. 3426[1] has been referred to several times and it has been intimated that calculations have been made by B.A.C. and Sud Aviation. We now discuss how the results of this Report relate to these previous investigations.

In the two-dimensional method of R. & M. 3426, spanwise deformability was ignored. It would be hoped, then, that consideration of the present results would indicate the extent to which spanwise deformability does in fact influence the behaviour of a 'Concorde'-like slender aircraft and also the variations in the effects of aeroelasticity with variations in the spanwise locations of the control surfaces. However, it must be remembered that the two sets of results relate not only to somewhat different aerodynamic configurations but also to two fundamentally dissimilar aircraft as regards structural stiffness characteristics. A quantitatively meaningful comparison is therefore not possible and we must be content with a discussion in qualitative terms.

It has already been seen that the effects of aeroelasticity vary markedly with the spanwise positions of the control surfaces and in Section 3.6.6 some physical explanation of this variation has been furnished by consideration of the elastic warp produced. This warp consists of spanwise bending together with an amount of wash-in or wash-out which differs with differing control gearings. There is only a small amount of curvature of chordwise sections. By contrast, the fact that in the two-dimensional approach there is no distortion of spanwise sections implies that the mode of deflection consists of curvature of chordwise sections together with wash-in or wash-out, of which the spanwise variation is, for practical layouts, quite gradual. There is, then, little similarity between the deflections calculated here and those presented in R. & M. 3426 and it seems that if an attempt were made to apply the two-dimensional approach to a 'Concorde'-like design there could be little confidence in the results obtained.

The two-dimensional approach predicted an increase due to aeroelasticity in the magnitude of the elevator angle per g; the magnitude of this increase became larger at higher kinetic pressures. The present results exhibit similar trends when only outboard controls are used. When all three controls are used the increment can be of either sign, depending on the mass distribution, and its magnitude can increase or decrease with increasing Q. The use of only inboard controls produces an increment such that the magnitude of the elevator angle per g is decreased by aeroelasticity: the increment itself decreases in magnitude with increasing Q. This progressive divergence from the trends exhibited by the two-dimensional results, as the control gearings are varied to decrease the contribution of the outboard controls, is consistent with the progressive development of elastic warp of a character very different from that of the two-dimensional mode of deflection.

A sounder basis for a direct comparison of the present results with earlier work is provided by an unpublished report of the British Aircraft Corporation which presents results of aeroelastic calculations for a configuration substantially the same as that considered here. In the B.A.C. investigation an 'assumed mode' approach was adopted, with aerodynamic loads due to distortion specified by influence coefficients derived by the method of Pines, Dugundji and Neuringer. The rectangular grid employed divided the planform into about 100 areas but did not extend over the whole of the forward fuselage. Structural characteristics were defined by a matrix of structural-stiffness influence coefficients for 121 points on the half-aircraft. Both the aerodynamic loads due to distortion and the structural characteristics were therefore defined in rather greater detail in the B.A.C. calculations than in those of this Report. In problems as complex as these, where accuracies are inherently difficult to determine, it is not very profitable to attempt to explain every apparent discrepancy between results achieved by different people using different methods. One can hope, however, for the absence of any gross discrepancies which would suggest a fundamental error in one or other of the methods, or some incidental errors of computation. Bearing such considerations in mind we may compare some of the results for the control angles to trim and to manoeuvre, as determined here and as determined by B.A.C. for the same rigid aircraft cg margins and (approximately) the same weights. (The fuel distributions assumed by B.A.C. are not known in detail.)

The results to be compared are presented in Tables 1 and 2.

The results for control angles per g (Table 2) are considered to indicate a good measure of agreement between the two investigations. In general, the B.A.C. results show a somewhat larger variation of the aeroelastic effects with control location.

The results for control angles to trim (Table 1) do not compare so satisfactorily, although it is to be noted that all the angles involved are quite small. The differences in the values of η_t for the rigid aircraft are largely attributable to a difference in the pitching moment at zero lift. The R.A.E. results consistently indicate smaller increases due to aeroelasticity in η_t. A possible explanation is that the Lees method, applied to the complete planform, overestimates the down load due to deflection of the nose and thus also overestimates the extent to which the destabilising moment due to elastic warp of the wing is counteracted by incremental down load on the nose. Such considerations underline the need for experimental substantiation of methods of determining the loading on slender configurations due to arbitrary distributions of elastic warp.

4. *The State of Development of the Method.*

The method presented here was first conceived when it became apparent that the neglect of spanwise deformability, implicit in the method of R. & M. 3426, was invalid for a 'Concorde'-like slender layout incorporating a thin wing in conjunction with a discrete fuselage. To provide a direct follow-up to the results of that report, the present method has been used to determine static aeroelastic effects on an early projected version of the 'Concorde' at its cruising Mach number of 2·2.

It has seemed worthwhile to develop the method in a general form and, with the help of the experience gained in an initial application, to consider its potentialities and the difficulties which must be overcome before it can become a practical design technique.

The principle of superposition has been employed so that linearity of the aircraft's structural and aerodynamic properties has been tacitly assumed. A fully three-dimensional description of these properties can be achieved by the matrix approach and so, in principle, the method is applicable to any aircraft, the structure of which is analysable in such a way that a flexibility influence matrix can be found, and for which there exist theories to provide the aerodynamic influence matrices. The theory has so far been developed in detail only for symmetric flight conditions; while there are apparently no difficulties of principle which would prevent its extension to more general conditions it is felt that the practical problems in its application would be quite formidable. In the subsequent discussion of the developments which are necessary we will therefore assume that we are seeking to establish the method as a design technique for symmetric flight conditions only.

In any method which employs discrete-element approximations for continuously varying quantities it is desirable to know the number and distribution of elements necessary to obtain an adequate approximation. Thus, in the present method, one wishes to be able to make appropriate choices of the sets of points to be used in the calculation of the structural and aerodynamic influence coefficients and the component loading systems. Some basic considerations are discussed in Appendix A, where it is suggested that extensive numerical investigations would be necessary to determine the optimum relationship between the sets and that, further, the most profitable choices for any particular problem might have to be found by numerical experiment. In the single application of the method conducted so far the matrix of aerodynamic coefficients was derived by 'hand' computation using the method of Lees[2]. Even for the modestly sized matrix used this was a tedious process so that although Lees's method appears potentially well suited to the task one would wish to programme it for automatic computation before attempting to use it systematically in the present method. A similar proviso could be attached to the incorporation of most other aerodynamic theories. Some of the other computations, involved in the derivation of the transformation matrices $\mathscr{C}$ and $\mathscr{F}$ and in the conversion of distributed loadings to point-load vectors, also proved rather laborious when performed by hand.

In view of the above, it appears that although the numerical work described in this Report has established the general practicability of the method it has not been extensive enough to develop it to the stage where it could be offered as a routine design procedure of immediate and universal applicability.

However, as far as the authors are aware, this stage has not been reached by any method currently available (in the U.K. at least): the tendency has been for designers to develop *ad hoc* procedures appropriate to their own particular problems. Thus, in an assessment of relative merits the present method would not suffer, on the score of incomplete development, in comparison with those used elsewhere. Indeed, it should have some advantage in that the general framework here described affords considerable scope for developing a fully automated and widely applicable method of assessing quasi-steady aeroelastic effects.

5. *Concluding Discussion.*

Early concepts of a slender near-delta supersonic transport aircraft involved designs which were to a large extent 'integrated', with the wing providing considerable volume and the fuselage being regarded as a lifting component. For this type of design the stiffness of spanwise sections would be large compared with that of lengthwise sections; therefore it could be considered plausible to ignore spanwise deformations and to make aeroelastic calculations on the assumption that the aircraft behaved as a beam, subject only to longitudinal bending. A method based upon this assumption was described in R. & M. 3426[1]. However, the layout selected for the Anglo-French 'Concorde' project features a thin wing in conjunction with a discrete fuselage and it was clear that for such an aircraft the neglect of spanwise deformations was not justified. Accordingly, it was necessary to formulate a 'three-dimensional' method of determining static aeroelastic effects. A matrix formulation of the problem was selected and the method was first developed in a general form and then somewhat specialised for its application to a 'Concorde'-like slender aircraft in symmetric flight at $M = 2{\cdot}2$.

The method is intended primarily for application at a fairly advanced stage of design. It is assumed that the stiffness characteristics of the structure and the mass distribution will then be specified in considerable detail, and that correspondingly detailed basic aerodynamic load distribution data will be available from experiment or theory. It is further assumed that the incremental aerodynamic loading due to deformation will be calculable, in the form of a matrix of influence coefficients, from a linearised theory appropriate to the configuration and flow regime under consideration. One may then make suitable choices of the various sets of points to be employed and derive the rigid aircraft load vectors, the structural flexibility and aerodynamic influence matrices, and their associated transformation matrices. Starting from this representation of the problem, the method is able to provide direct solutions which are 'exact' within the limits of accuracy of the computing processes employed. In this respect it is superior to alternative methods which usually involve iteration or the adoption of a limited number of assumed modes of deformation. As regards computational economy the present method, in a fully automated form, should compare favourably with its rivals.

Results of the numerical application to a slender supersonic transport aircraft have been presented and discussed. They include the calculated incidences and control angles to trim and to sustain quasi-steady manoeuvres, the longitudinal distributions of shear force and bending moment, and the deformation (elastic warp) of the aircraft.

As calculated by the present method, all of the effects in question are quite unspectacular at flight-plan values of the kinetic pressure. The trim and manoeuvrability results reveal no tendency towards control reversal up to kinetic pressures well in excess of these values. The spanwise position of the control surfaces has a marked effect; in the case of outboard controls the elevator angle per g is increased by aeroelasticity whereas in the case of inboard controls it is reduced. These results are consistent with the elastic warp produced. When only outboard controls are used there is little wash-in or wash-out, the mode of deflection consisting mainly of spanwise bending together with a downward deflection of the nose, whilst the use of only inboard controls produces a pronounced curling-up at the wing tips, i.e. the spanwise bending is combined with considerable wash-out of the outer parts of the wing. The longitudinal distributions of shear force and bending moment are little affected by aeroelasticity: the maximum value of the latter has been increased in the $2{\cdot}5g$ case by up to about 5 per cent.

Comparison with the results of R. & M. 3426 shows that the 'two-dimensional' method presented there is not applicable to a 'Concorde'-like design and may give completely misleading results, especially

when inboard control surfaces are used. A comparison with the results of an investigation by B.A.C. for a very similar design, but using a different technique, shows that the two sets of results agree well as regards the elevator angles per g but exhibit differences in the elevator angles to trim.

This Report, wherein the principles behind the method are expounded and a preliminary application is described, marks the completion of the first phase of the method's development. From the remarks made earlier in this discussion and in Section 4 it is concluded that the potentialities of the method are sufficient to justify the expenditure of the further effort which would be necessary to develop it into a routine design tool with wide applicability. Automation of many of the processes involved would be the next obvious step, since this would make possible an extensive application of the method to a variety of designs and flight conditions. Only in this way could the potentialities of the method be assessed.

LIST OF SYMBOLS

Note:

(i) Loads, incidences etc. are defined at discrete points. Suppose that all sets of such points are numbered as they are introduced; then we denote the rth set by Σ_r and the number of points in Σ_r by n_r. A typical member of *any* set of quantities is indicated by the suffix i. Hence from the symbol A_i, say, we cannot deduce which set of points contains the point where A_i is defined, nor does the suffix i indicate any particular point in a set. Thus the various suffices i in any sentence or matrix equation are unrelated.

(ii) A column vector of quantities defined at the points of the set Σ_r (or 'in Σ_r') is denoted by $\{A_i\}_r$, for example.

(iii) Matrices, with the exception of column vectors, are denoted by script characters, e.g. $\mathscr{S}$.

(iv) In the following list all symbols refer to quantities appropriate to the flexible aircraft: the corresponding rigid aircraft quantities are denoted by a superscribed bar, e.g. $\bar{Q}_i$ from Q_i.

C_L Lift coefficient

L_i Load at a point of Σ_2: lb

M Mach number

$M(x)$ Longitudinal distribution of bending moment: lb ft

M_C, M_F etc. Moments about moment reference station corresponding to component loadings $\{Q_i\}_1^C$, $\{Q_i\}_1^F$, etc.

P_i Incremental load due to elastic warp at a point of Σ_3: lb

$Q = \frac{1}{2}\rho V^2$ Kinetic pressure: lb/ft^2

Q_i Load at a point of Σ_1: lb

Q_i^D Value of Q_i at the design point

$\Delta Q_i = Q_i - \bar{Q}_i$ Increment in load due to aeroelasticity: lb

$\{Q_i\}_1^C$ Vector of aerodynamic loads for $C_L = 0{\cdot}1$: lb/Q

$\{Q_i\}_1^F$ Vector of inertial loads due to fuel (per g): lb

$\{Q_i\}_1^I$ Vector of inertial loads for the aircraft with zero fuel (per g): lb

$\{Q_i\}_1^W$ Vector of aerodynamic loads due to compensatory warp: lb/Q

$\{Q_i\}_1^q$ Vector of aerodynamic loads due to rate of pitch (per incremental g): lb/Q

$\{Q_i\}_1^\alpha$ Vector of aerodynamic loads due to incidence (per radian): lb/Q

$\{Q_i\}_1^\eta$ Vector of aerodynamic loads due to elevator deflection (per radian): lb/Q

$S(x)$ Longitudinal distribution of shear force: lb

V Speed of flight: ft/sec

W Aircraft mass: lb

Z_C, Z_F, etc. Total loads due to loading systems $\{Q_i\}_1^C$, $\{Q_i\}_1^F$ etc.

a_r Coefficient of rth component loading (equation (13))

c_0 Reference chord: ft

g_r Gearing of rth control

k_r Ratio of amount of fuel in rth tank to maximum capacity of tank

n		Total normal-acceleration coefficient
n_r		Number of points in Σ_r
q		Rate of pitch: rad/sec
x		Distance aft of nose of aircraft: ft
x_i		Distance of a general point aft of nose of aircraft: ft
x_i'		Distance of a general point ahead of moment reference station: ft
$\bar{x}$		Distance of centre of gravity ahead of moment reference station: ft
w_i		Deflection at a point of Σ_2: ft
w_i^D		Value of w_i for design-point loading
$\mathscr{C}$		Transformation matrix between α_i and w_i (equation (6))
$\mathscr{E}$		Transformation matrix between L_i and Q_i (equation (3))
$\mathscr{F}$		Transformation matrix between ΔQ_i and P_i (equation (7))
$\mathscr{I}$		Unit matrix
$\{\mathscr{I}_i\}_4$		Unit column vector in Σ_4
$\mathscr{L}$		Matrix product $\mathscr{F}\mathscr{R}\mathscr{C}\mathscr{S}\mathscr{E}$
$\mathscr{R}$		Aerodynamic influence matrix
$\mathscr{R}^*$	$=$	$\mathscr{R}/Q$
$\mathscr{S}$		Structural flexibility influence matrix
Σ_r		rth set of points
α		Incidence: rad
α_i		Elastic incidence at a point of Σ_4
α_t		Value of α for $n = 1{\cdot}0$
η		Elevator deflection: rad
η_t		Value of η for $n = 1{\cdot}0$

REFERENCES

No.	*Author(s)*	*Title, etc.*
1	A. S. Taylor and W. F. W. Urich	Effects of longitudinal elastic camber on slender aircraft in steady symmetrical flight: Parts I and II. A.R.C. R. & M. 3426 (1964).
2	D. E. Lees	Aerodynamic influence coefficients for delta wings in steady supersonic flow. *Aircraft Engineering, 31,* No. 359, 9–12 (1959).
3	D. Williams	Solution of aeroelastic problems by means of influence coefficients. R.A.E. Report Structures 169 (1954). A.R.C. 17439.
4	E. G. Broadbent	The rolling power of an elastic swept wing. A.R.C. R. & M. 2857 (1954).
5	J. J. Foody and L. Reid ..	The solution of aeroelastic problems on wings of arbitrary planform by matrix methods. *J. R. aero. Soc., 59,* No. 540, 843–846 (1955).
6	W. A. Tucker and R. L. Nelson	Characteristics of thin triangular wings with constant-chord partial-span control surfaces at supersonic speeds. NACA TN 1660 (1948).
7	G. T. S. Done	Interpolation of mode shapes: a matrix scheme using two-way spline curves. *Aeronautical Quarterly, XVI,* Part 4, 333–348 (1965).

APPENDIX A

On Choosing the Sets of Points Σ_r.

Fundamentally, one desires to choose the sets of points Σ_r so that a certain accuracy may be achieved with the greatest overall computational economy. In practice, the pursuance of this goal in any given case is made difficult by the existence of features peculiar to that case, including the aircraft's configuration and the methods selected for performing aerodynamic and structural analyses, as well as by the freedom of choice which one has at several points in the procedure. Detailed discussion of such topics is beyond the scope of this Report and we content ourselves with discussing in this Appendix some of the factors which determine the accuracy of the present method and deriving some basic principles which guide the choices of the various sets of points employed.

Since the net loading on a free-flying aircraft is a combination of various locally additive or subtractive load systems, it is virtually impossible to assess the general standard of accuracy attainable in its estimation. Clearly, however, the accuracy of this net loading will improve as the accuracies of its components improve and therefore it is both convenient and instructive to consider the accuracy of an arbitrary individual loading system. In all that follows, three assumptions are made:

(i) The load system on the hypothetical rigid aircraft is known precisely.

(ii) By taking a sufficiently large aerodynamic influence matrix, the load due to elastic warp may be derived as accurately as we please.

(iii) An analysis of the aircraft structure, idealised in some way, has provided a matrix $\mathscr{S}^*$ of flexibility influence coefficients for a set of points $\Sigma_2{}^*$. The matrix $\mathscr{S}$ will be formed by selecting a sub-matrix of $\mathscr{S}^*$ comprising the rows and columns corresponding to a subset, Σ_2, of $\Sigma_2{}^*$.

We recall that an individual loading system for the flexible aircraft, $\{Q_i\}_1^r$, is derived from the corresponding system for the rigid aircraft, $\{\bar{Q}_i\}_1^r$, by the addition of a system of aerodynamic loads due to elastic warp, $\{\Delta Q_i\}_1^r$ (equation (1)). The accuracy in $\{Q_i\}_1^r$ is most easily discussed by retracing the steps through which $\{\Delta Q_i\}_1^r$ is determined. That is, we recapitulate the steps of the method, as given in Section 2, but in 'reverse' order. The steps are

(a) The derivation of loads in Σ_1 from loads in Σ_3, using matrix $\mathscr{F}$.

(b) The derivation of loads in Σ_3 from incidences in Σ_4, using matrix $\mathscr{R}$.

(c) The derivation of incidences in Σ_4 from deflections in Σ_2, using matrix $\mathscr{C}$.

(d) The derivation of deflections in Σ_2 from loads in Σ_2, using matrix $\mathscr{S}$.

(e) The derivation of loads in Σ_2 from loads in Σ_1, using matrix $\mathscr{E}$.

We now consider each of these in turn.

(a) A fundamental point is that Σ_1 must cover the whole of the region of the aircraft which is covered by Σ_3. In the example presented in this Report the various sets of points are common to all the calculations of the aeroelastic modifications to individual loading systems, and each set covers the whole aircraft. However, in cases where an aircraft could be considered as consisting of discrete components, such as the 'classical' fairly high aspect ratio, tailed aircraft, certain load systems would act over only a part of the aircraft and cause significant load due to elastic warp over only a part. It might then be profitable to use different sets of points for different loading systems. For any system, Σ_3 must cover the part of the aircraft where deflections cause significant loads and so Σ_1 must also cover this area. Thus, for instance, for the aircraft considered here, the rigid aircraft load due to control deflection acts only on the part rearward of the hinge line (at supersonic speeds) but a set Σ_1 which covered only this area would be inadequate.

Also, it can be seen that the density of points in Σ_3 should be at least as high as in Σ_1 since otherwise there is a degree of indeterminateness in transforming the loads in Σ_3 to loads in Σ_1.

(b) The set Σ_3 which is necessary to determine the load due to elastic warp with the required accuracy and detail is dependent on the aerodynamic theory employed, the aircraft configuration and, possibly, on the mode of deflection. The choice of Σ_3 is the central step which determines the accuracy which will be obtained, and which guides the choices of Σ_1 and Σ_2.

(c) The choice of a Σ_3, associated with a particular aerodynamic theory, fixes a corresponding Σ_4. Then the choice of Σ_2 depends on the requirement that one can determine the incidences in Σ_4 sufficiently accurately from the deflections in Σ_2. This may be influenced by the technique employed to derive the incidences. In the method used here they are derived from the deflections at neighbouring points and there is no attempt to deduce the overall deflected shape of the aircraft during this process. An alternative technique would be to find this overall shape by curve or surface fitting, by a method such as that of Done[7], and from it deduce the local incidences.

(d) Consider two influence matrices $\mathscr{S}$ and $\mathscr{S}'$ corresponding to sets of points Σ_2 and Σ_2', such that Σ_2' contains Σ_2 as a subset. Then if the loading were in fact a set of point loads in Σ_2 the deflections at the points of Σ_2 would, by assumption (iii) above, be the same whether they were calculated by using $\mathscr{S}$ or $\mathscr{S}'$. We may, then, say that this step alone does not introduce any errors in addition to those inherent in the structural analysis for the aircraft and those produced by the approximation to the distributed loading by a set of point loads in a particular Σ_2.

(e) To avoid introducing indeterminateness in the transformation of loads in Σ_1 to loads in Σ_2, the density of points in Σ_1 should be at least as high as in Σ_2.

From the foregoing discussion we see that, from considerations of the transformation of loadings, Σ_3 should be at least as dense as Σ_1 which should itself be at least as dense as Σ_2. However, the density of Σ_2 has a lower limit dictated by step (c).

It is clear that, even for a given configuration, in a fairly narrow band of flight conditions, much work is needed before one can determine the most appropriate choices of the various sets of points. As regards the choice of Σ_3, a large body of calculations performed for various Σ_3's (within a single aerodynamic theory) and for various configurations could indicate the accuracy in step (b) alone. Although in principle this step determines the accuracy of the whole process, one still has a good deal of freedom in choosing Σ_1 and Σ_2. It is possible that an extensive investigation on fairly general lines could provide a clearer indication of the optimum relationships between the sets of points. However, it is suspected that one would still be only part way to determining the most suitable sets for any particular problem. The feasibility of the routine use of the method may well depend on the success of attempts to provide a highly automated computational process which would allow one to investigate, by simple numerical experiment, the most profitable choices.

TABLE 1

Comparison of R.A.E. and B.A.C. Results for Elevator Angle to Trim at $M = 2{\cdot}2$.

Flight conditions: start of cruise; $W \approx 190\,000$ lb, $Q \approx 670$ lb/ft^2, rigid aircraft cg margin $0{\cdot}049c_0$.

Control gearings		B.A.C.	R.A.E.
$g_1 = g_2 = g_3 = 1{\cdot}0$ (All controls)	(η_t) rigid	$-0{\cdot}75°$	$0{\cdot}80°$
	(η_t) flexible	$+0{\cdot}75°$	$1{\cdot}36°$
	$\Delta\eta_t$ due to flexibility	$1{\cdot}50°$	$0{\cdot}56°$
$g_1 = 0, g_2 = g_3 = 1{\cdot}0$ (Outboard controls only)	(η_t) rigid	$-1{\cdot}15°$	$1{\cdot}30°$
	(η_t) flexible	$+1{\cdot}43°$	$2{\cdot}75°$
	$\Delta\eta_t$ due to flexibility	$2{\cdot}58°$	$1{\cdot}45°$
$g_1 = 1{\cdot}0, g_2 = g_3 = 0$ (Inboard controls only)	(η_t) rigid	$-2{\cdot}30°$	$2{\cdot}10°$
	(η_t) flexible	$+1{\cdot}26°$	$2{\cdot}75°$
	$\Delta\eta_t$ due to flexibility	$3{\cdot}56°$	$0{\cdot}65°$

TABLE 2

Comparison of R.A.E. and B.A.C. Results for Elevator Angle per g at $M = 2{\cdot}2$.

Control gearings	Flight conditions:	Start of cruise: $W \approx 190\,000$ lb, $Q \approx 670$ lb/ft^2 Rigid aircraft cg margin $0{\cdot}049c_0$		End of cruise: $W \approx 152\,000$ lb, $Q \approx 455$ lb/ft^2 Rigid aircraft cg margin $0{\cdot}052c_0$	
		B.A.C.	R.A.E.	B.A.C.	R.A.E.
$g_1 = g_2 = g_3 = 1{\cdot}0$ (All controls)	$(d\eta°/dn)$ rigid	−4·47	−4·07	−5·7	−5·08
	$(d\eta°/dn)$ flexible	−4·30	−3·83	−6·18	−5·52
	Ratio (flexible/rigid)	0·962	0·94	1·084	1·087
$g_1 = 0, g_2 = g_3 = 1{\cdot}0$ (Outboard controls only)	$(d\eta°/dn)$ rigid	−6·88	−6·6	−8·77	−8·25
	$(d\eta°/dn)$ flexible	−9·17	−7·7	−11·58	−10·3
	Ratio (flexible/rigid)	1·33	1·165	1·32	1·249
$g_1 = 1{\cdot}0, g_2 = g_3 = 0$ (Inboard controls only)	$(d\eta°/dn)$ rigid	−12·2	−10·6	−15·37	−13·2
	$(d\eta°/dn)$ flexible	−8·13	−7·6	−13·1	−11·9
	Ratio (flexible/rigid)	0·667	0·717	0·852	0·901

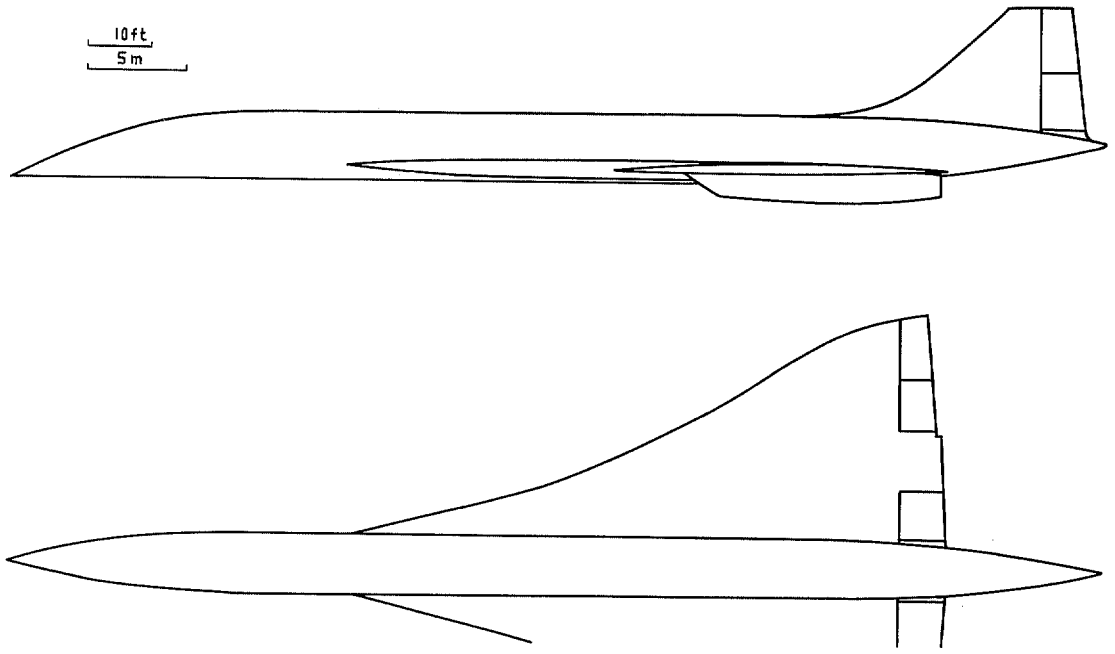

FIG. 1. General arrangement of the aircraft.

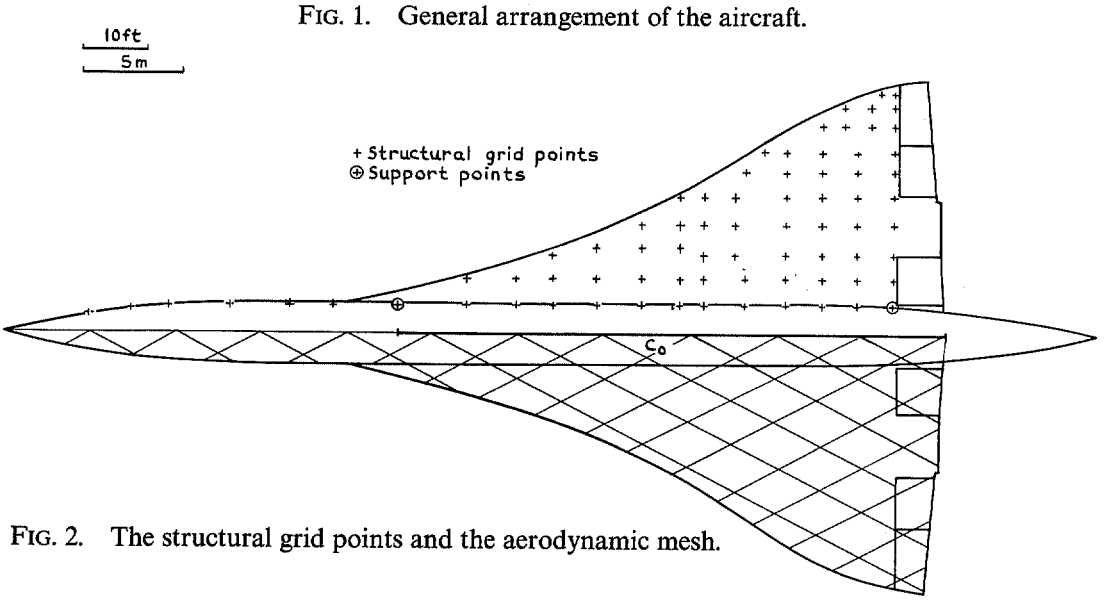

FIG. 2. The structural grid points and the aerodynamic mesh.

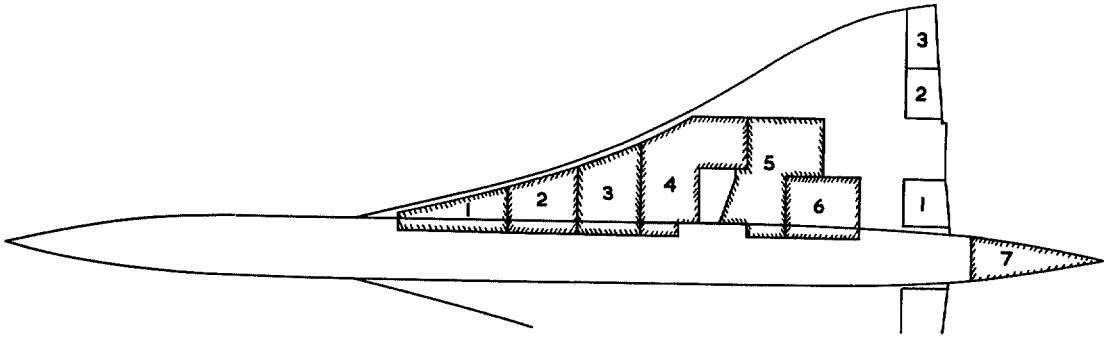

FIG. 3. Arrangement and numbering of the fuel tanks and elevators.

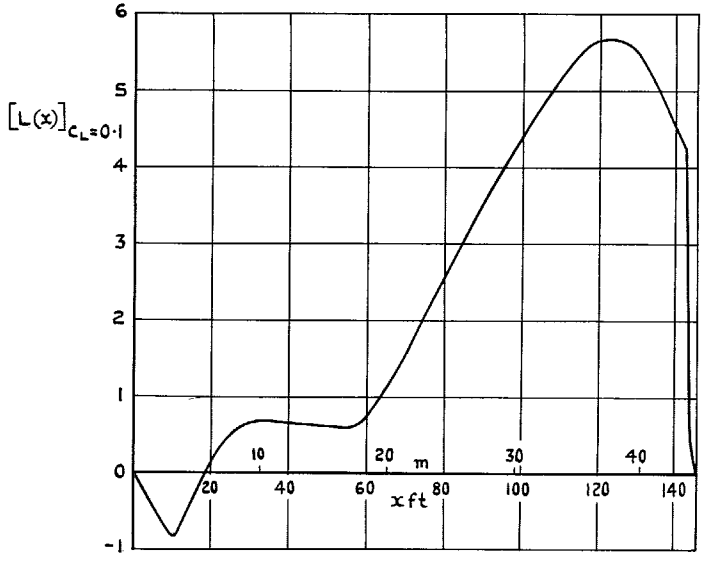

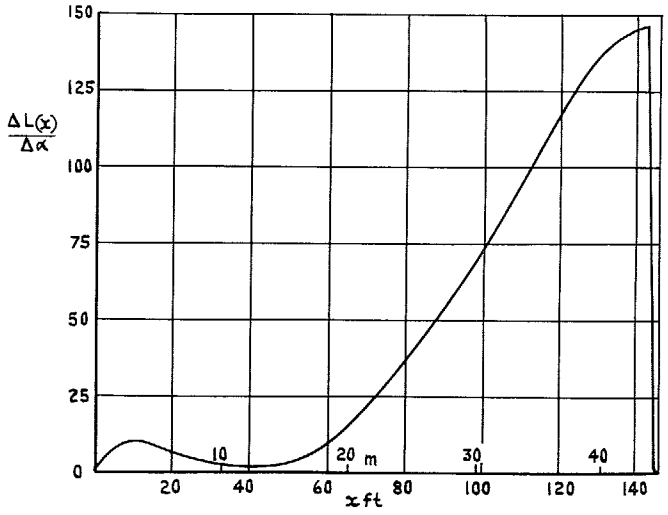

FIG. 4. Lengthwise distribution of aerodynamic loading components.

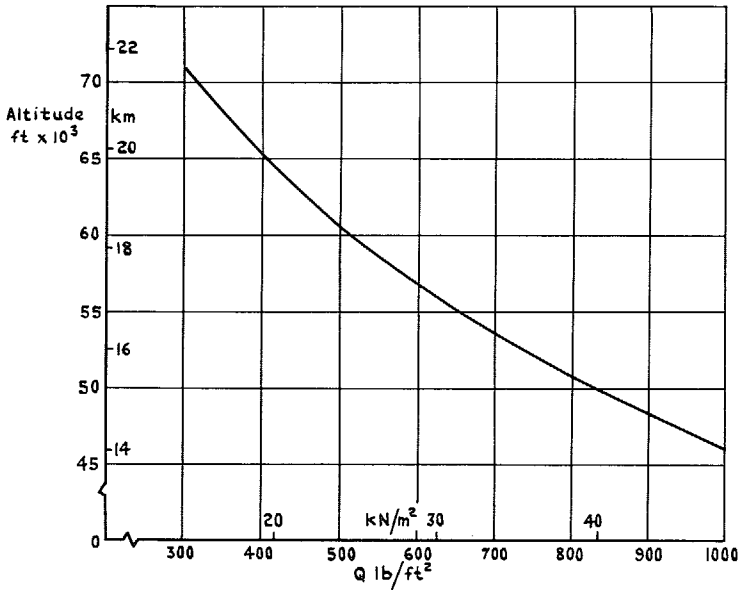

FIG. 5. Altitude *versus* kinetic pressure, $M = 2{\cdot}2$.

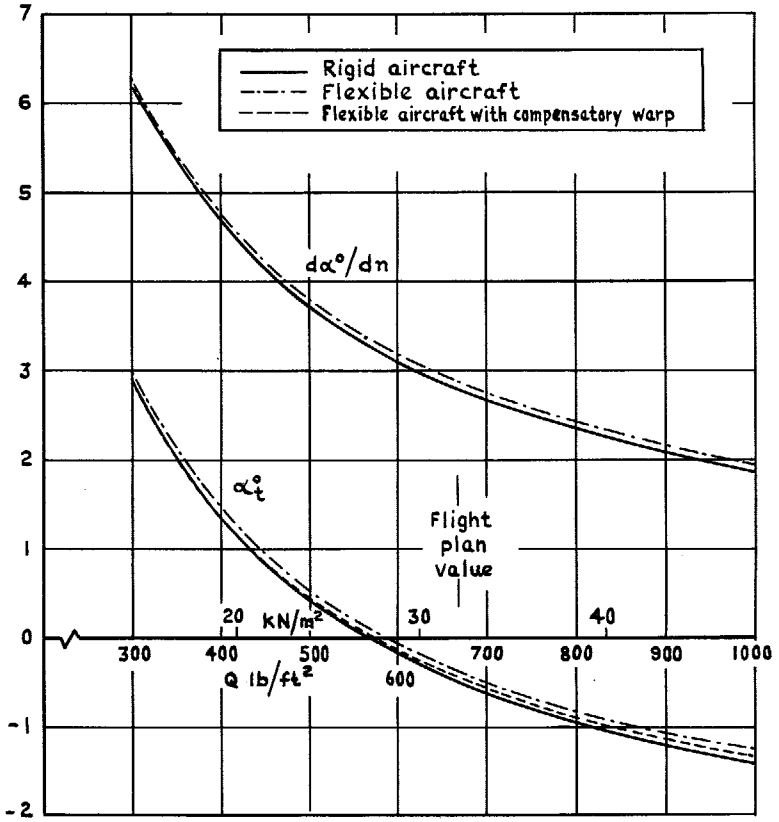

FIG. 6. α_t and $d\alpha/dn$. 'Start of cruise' fuel, $g_1 = 0$, $g_2 = g_3 = 1{\cdot}0$ for α_t; $g_1 = 1{\cdot}0$, $g_2 = g_3 = 0$ for $d\alpha/dn$.

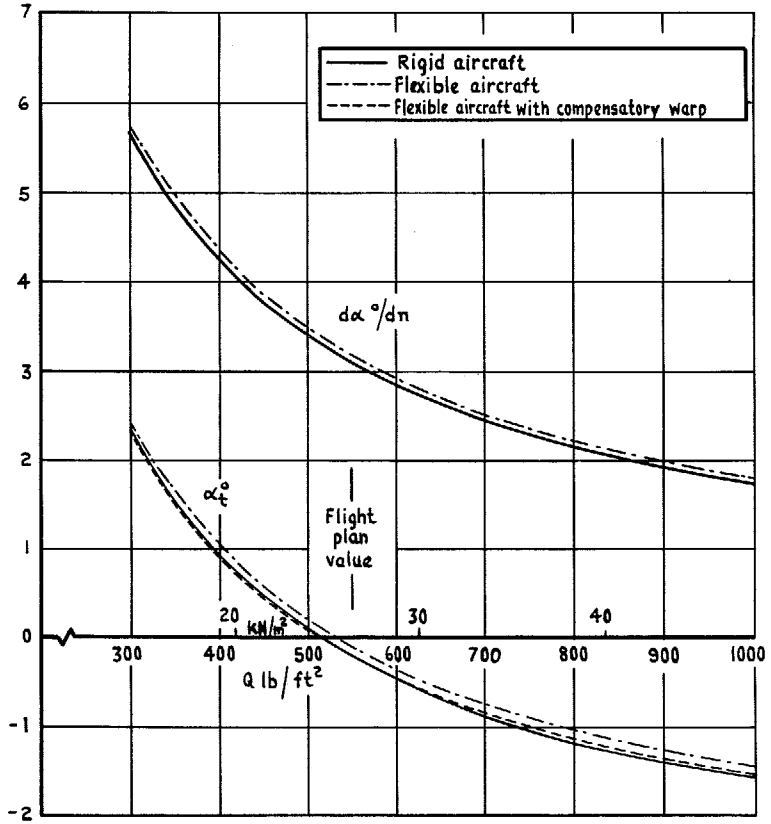

FIG. 7. α_t and $d\alpha/dn$. 'Design point' fuel, $g_1 = 0$, $g_2 = g_3 = 1{\cdot}0$, for α_t; $g_1 = 1{\cdot}0$, $g_2 = g_3 = 0$ for $d\alpha/dn$.

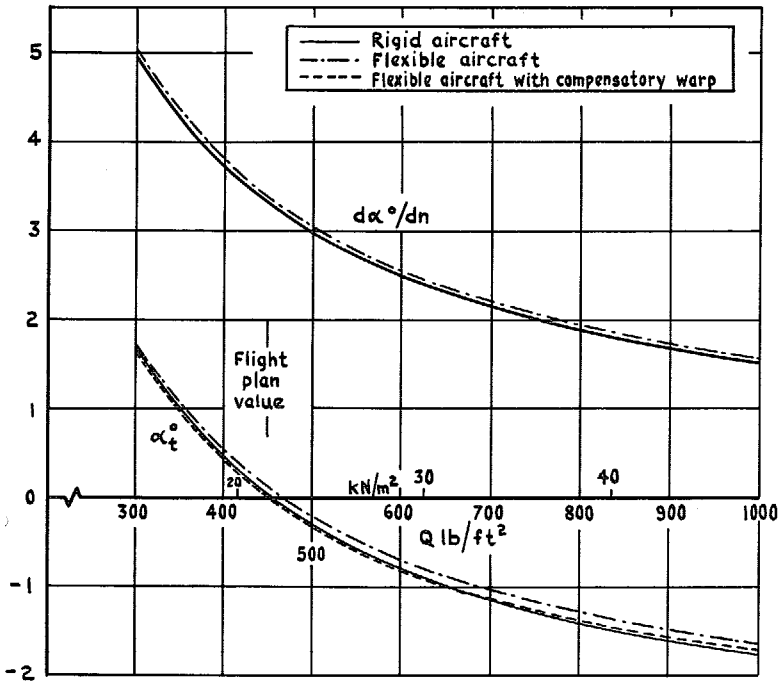

FIG. 8. α_t and $d\alpha/dn$. 'End of cruise' fuel, $g_1 = 0$, $g_2 = g_3 = 1{\cdot}0$, for α_t; $g_1 = 1{\cdot}0$, $g_2 = g_3 = 0$ for $d\alpha/dn$.

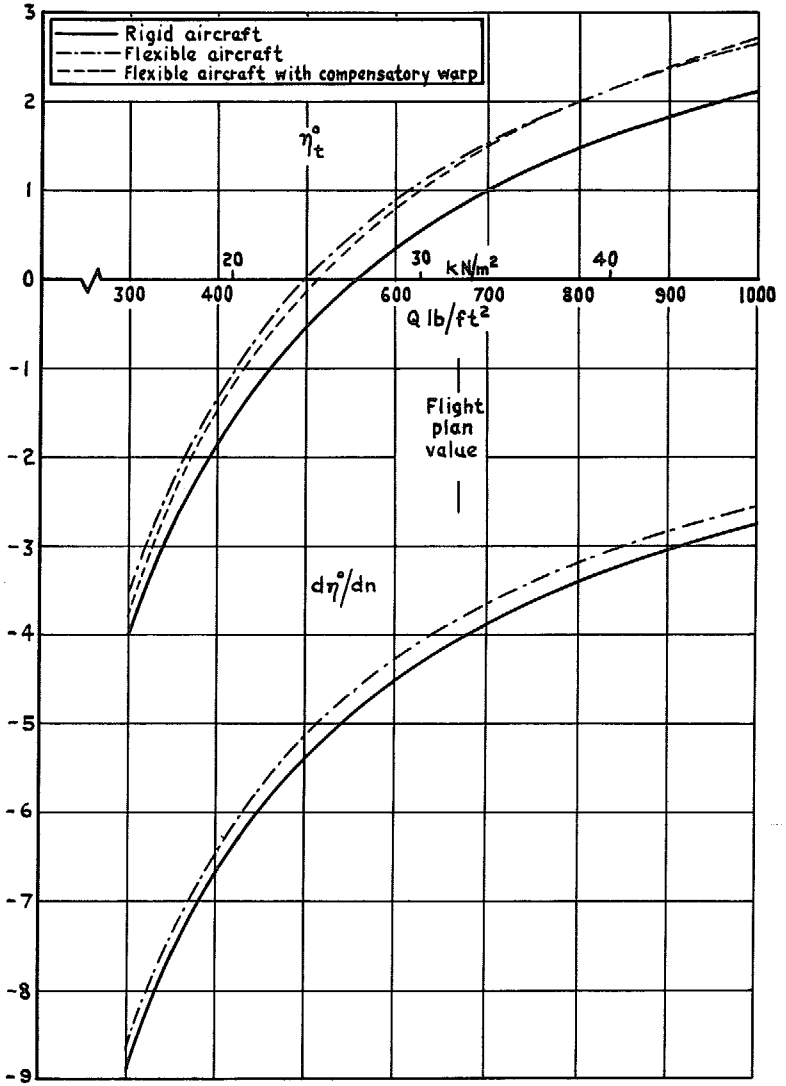

FIG. 9. η_t and $d\eta/dn$. $g_1 = g_2 = g_3 = 1{\cdot}0$, 'start of cruise' fuel.

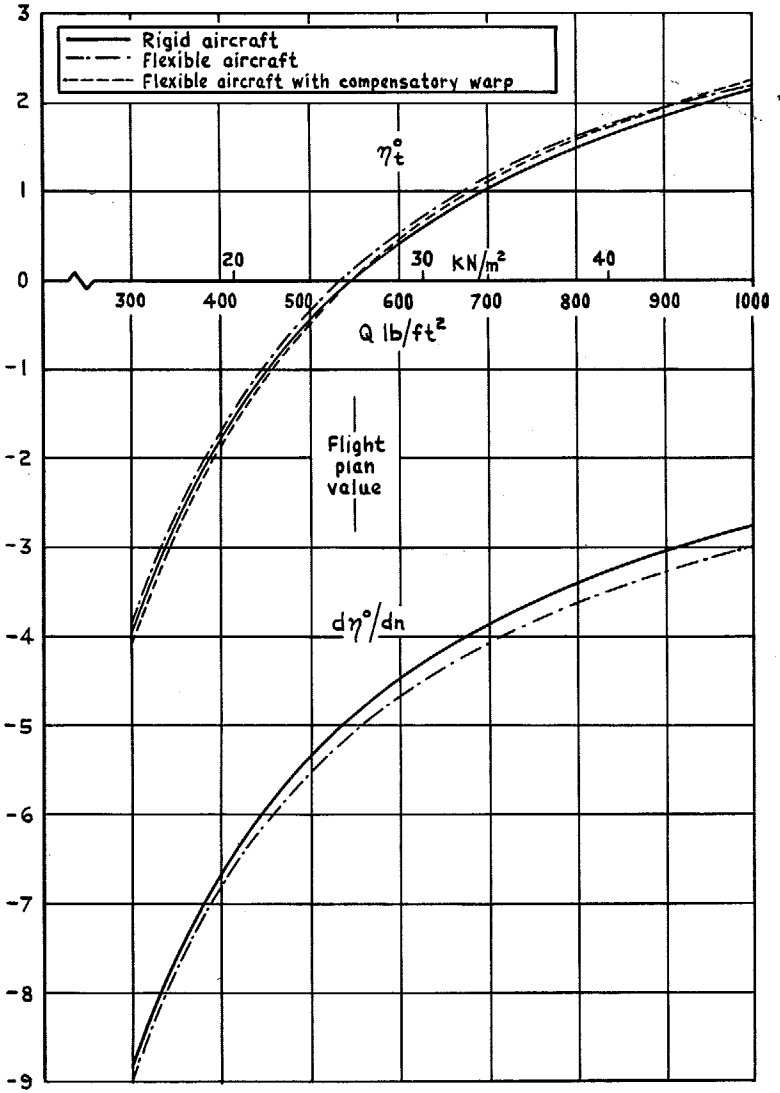

FIG. 10. η_t and $d\eta/dn$. $g_1 = g_2 = g_3 = 1{\cdot}0$, 'design point' fuel.

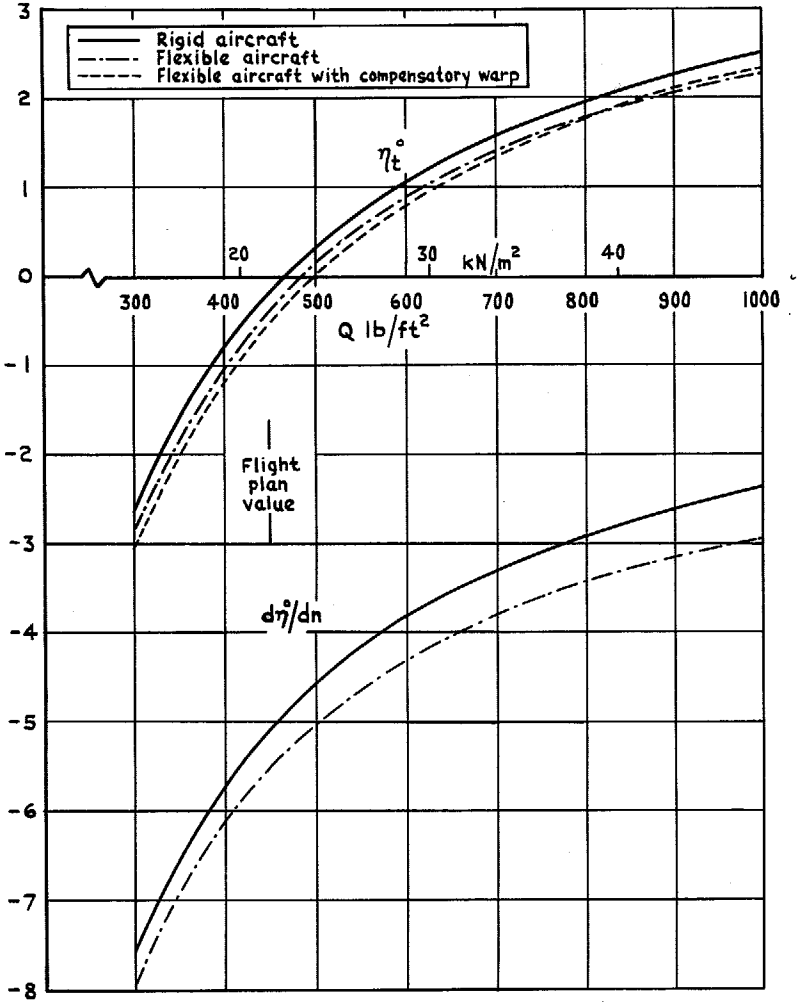

FIG. 11. η_t and $d\eta/dn$. $g_1 = g_2 = g_3 = 1{\cdot}0$, 'end of cruise' fuel.

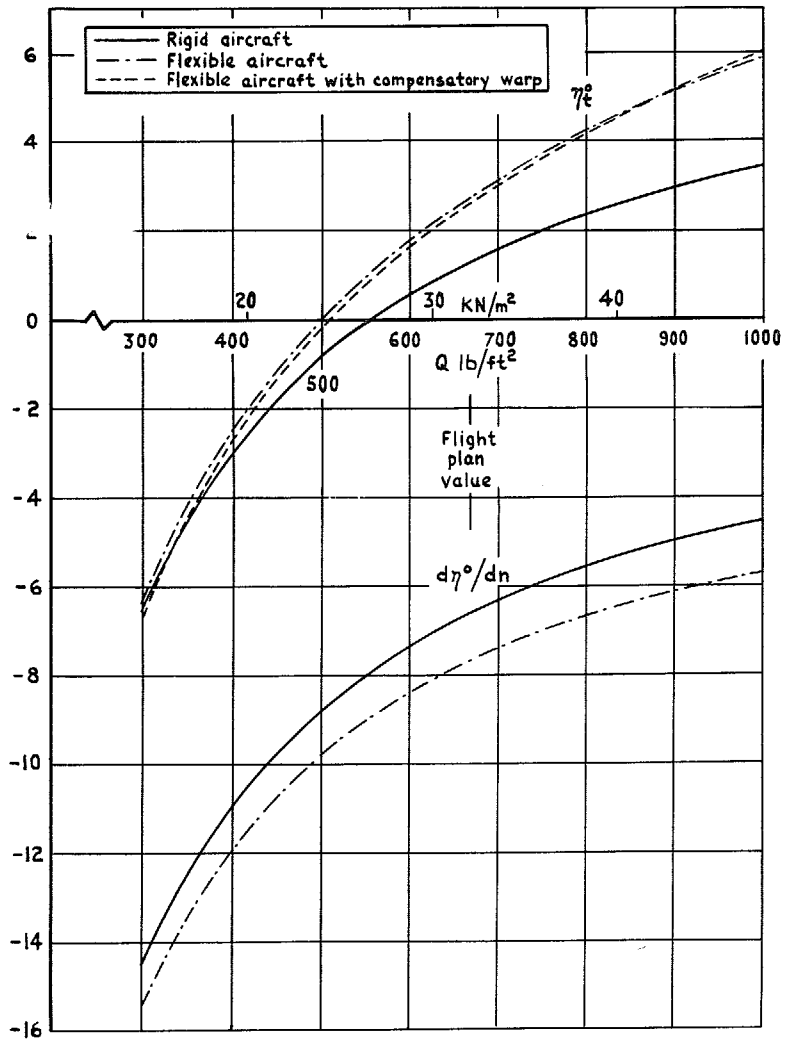

FIG. 12. η_t and $d\eta/dn$. $g_1 = 0, g_2 = g_3 = 1{\cdot}0$, 'start of cruise' fuel.

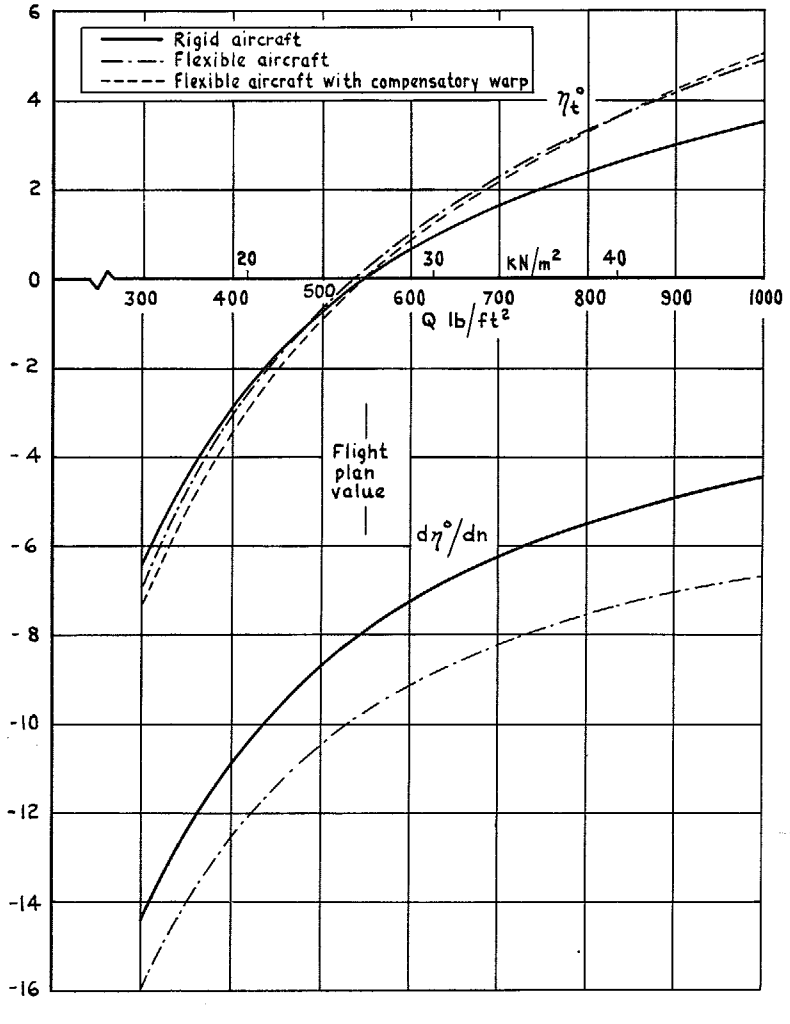

FIG. 13. η_t and $d\eta/dn$. $g_1 = 0$, $g_2 = g_3 = 1{\cdot}0$, 'design point' fuel.

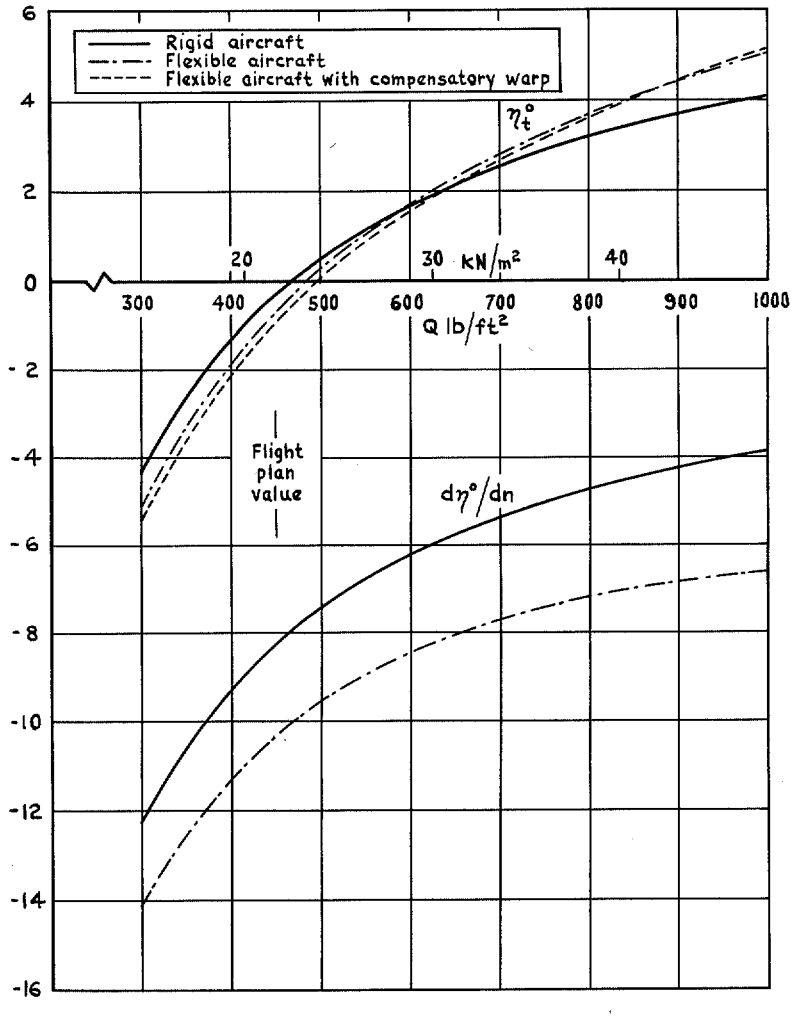

FIG. 14. η_t and $d\eta/dn$. $g_1 = 0, g_2 = g_3 = 1{\cdot}0$, 'end of cruise' fuel.

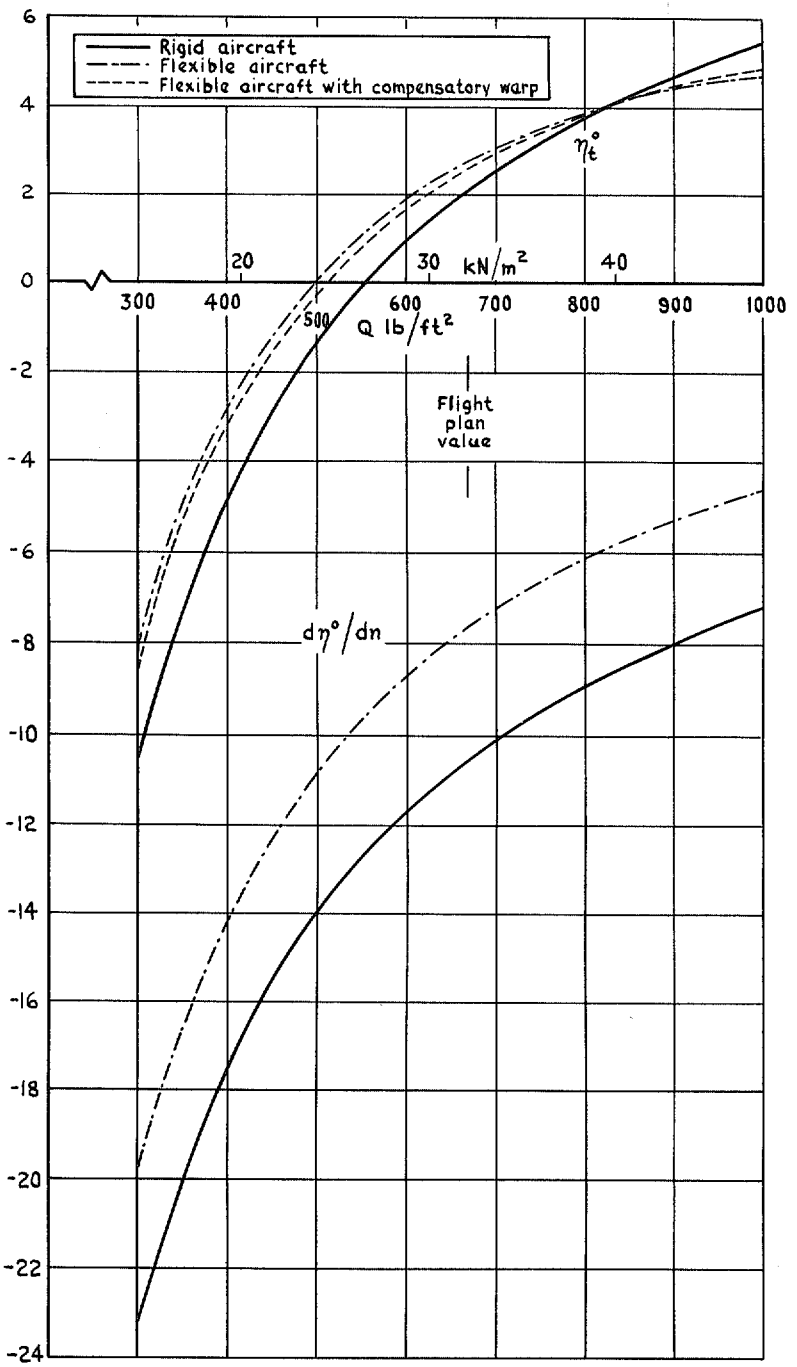

FIG. 15. η_t and $d\eta/dn$. $g_1 = 1{\cdot}0$, $g_2 = g_3 = 0$, 'start of cruise' fuel.

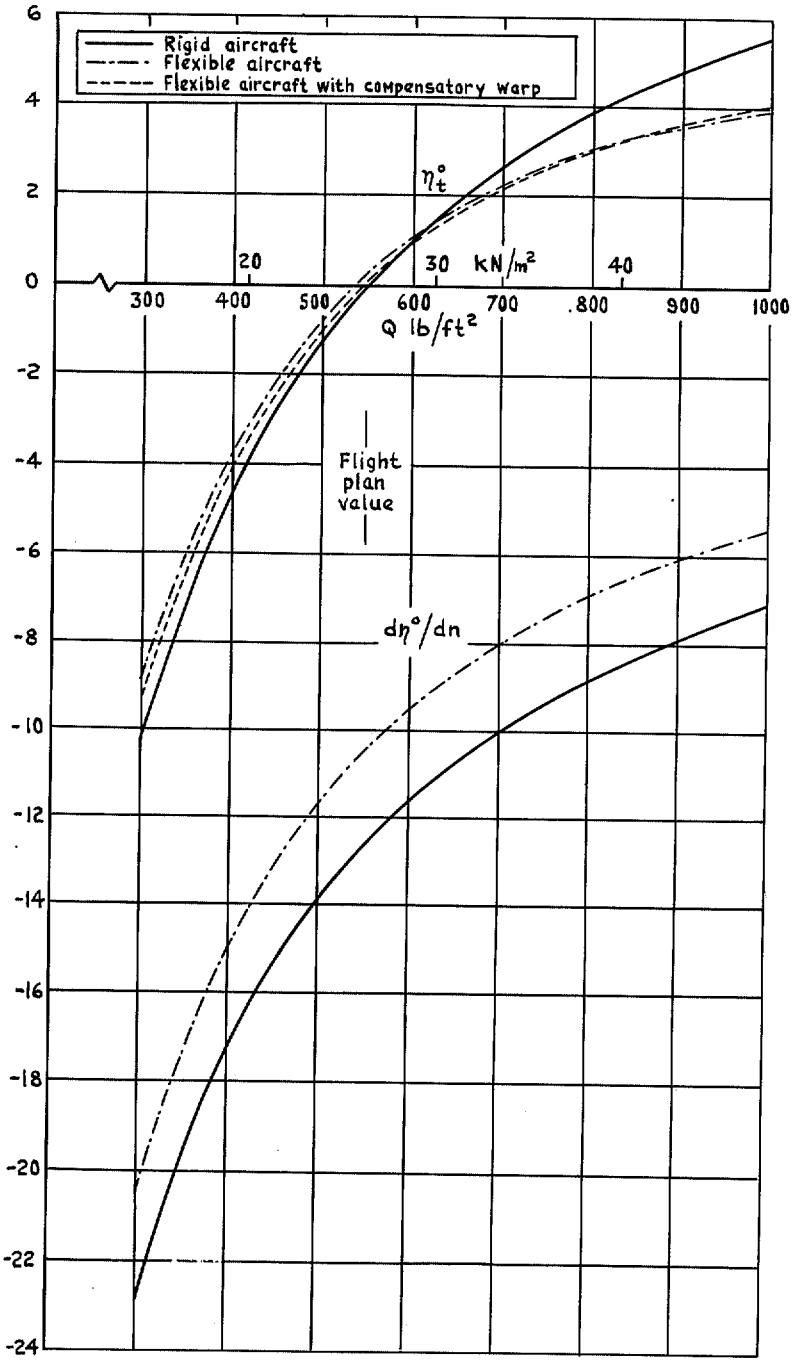

FIG. 16. η_t and $d\eta/dn$. $g_1 = 1{\cdot}0$, $g_2 = g_3 = 0$, 'design point' fuel.

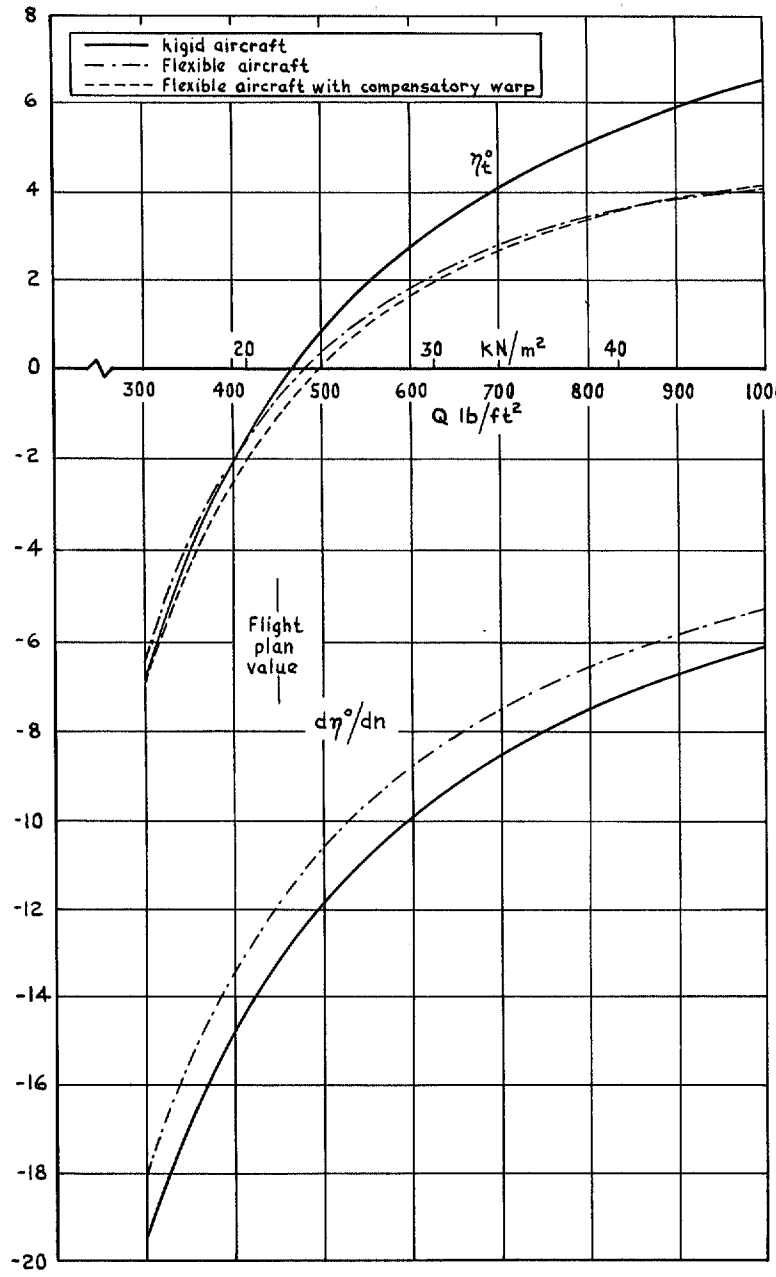

FIG. 17. η_t and $d\eta/dn$. $g_1 = 1{\cdot}0$, $g_2 = g_3 = 0$, 'end of cruise' fuel.

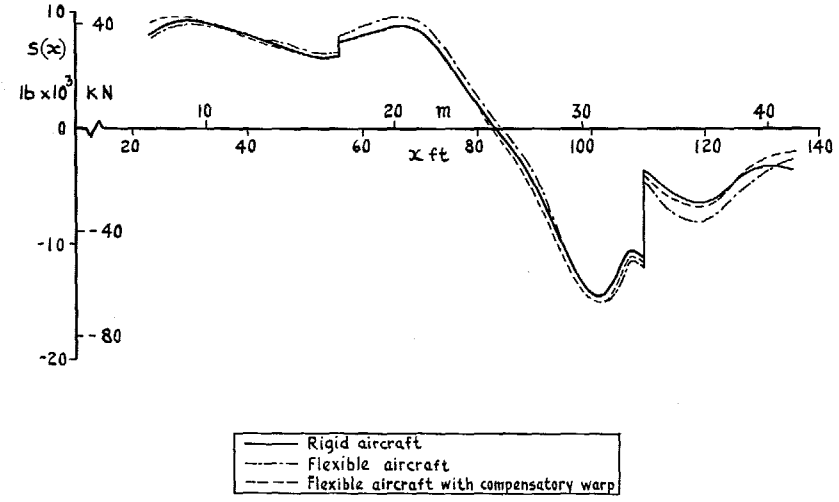

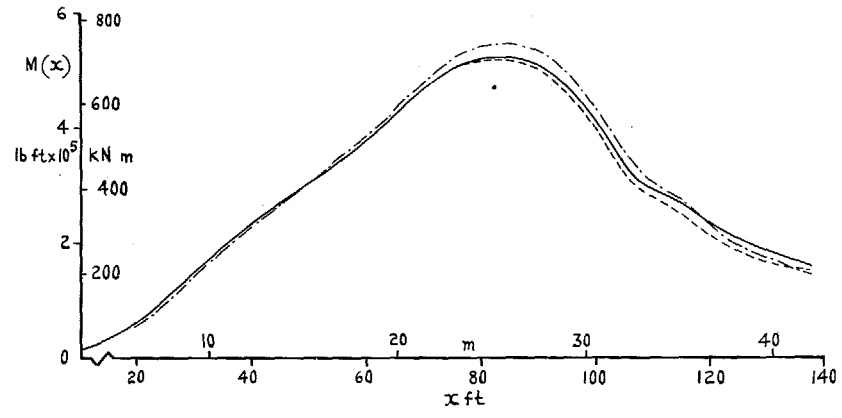

FIG. 18. Longitudinal distributions of shear force and bending moment. 'Start of cruise' fuel, $g_1 = g_2 = g_3 = 1{\cdot}0$, $Q = 670$ lb/ft^2, $n = 1{\cdot}0$.

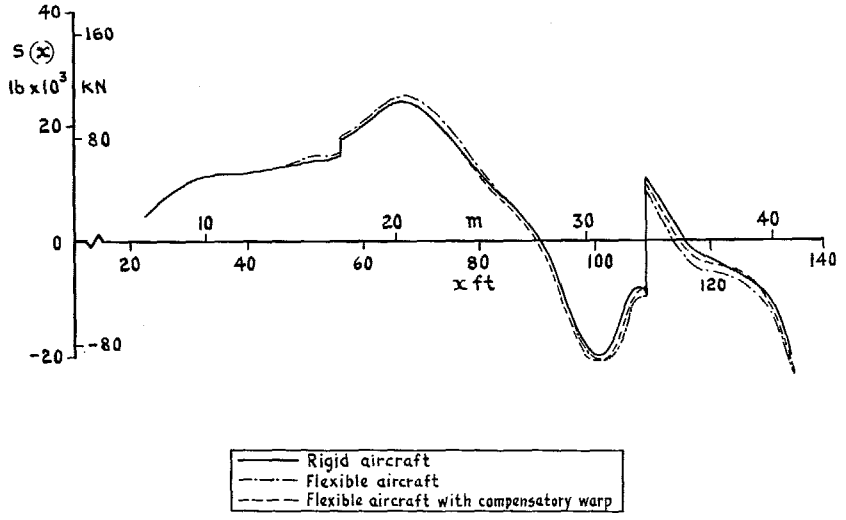

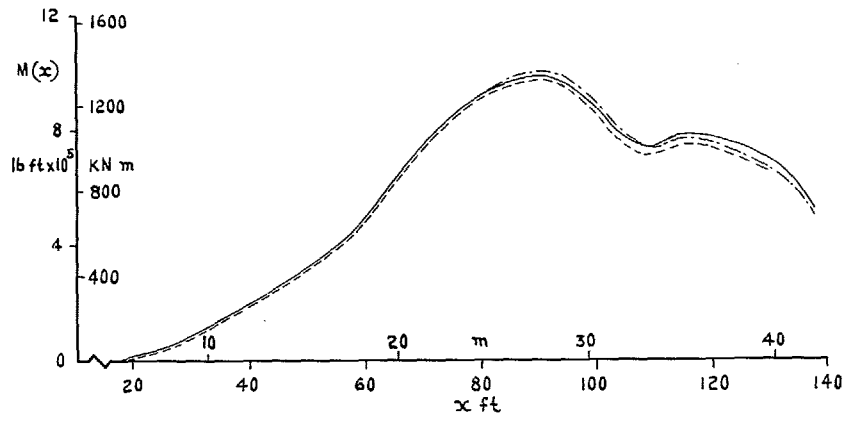

FIG. 19. Longitudinal distributions of shear force and bending moment. 'Start of cruise' fuel, $g_1 = g_2 = g_3 = 1{\cdot}0$, $Q = 670$ lb/ft^2, $n = 2{\cdot}5$.

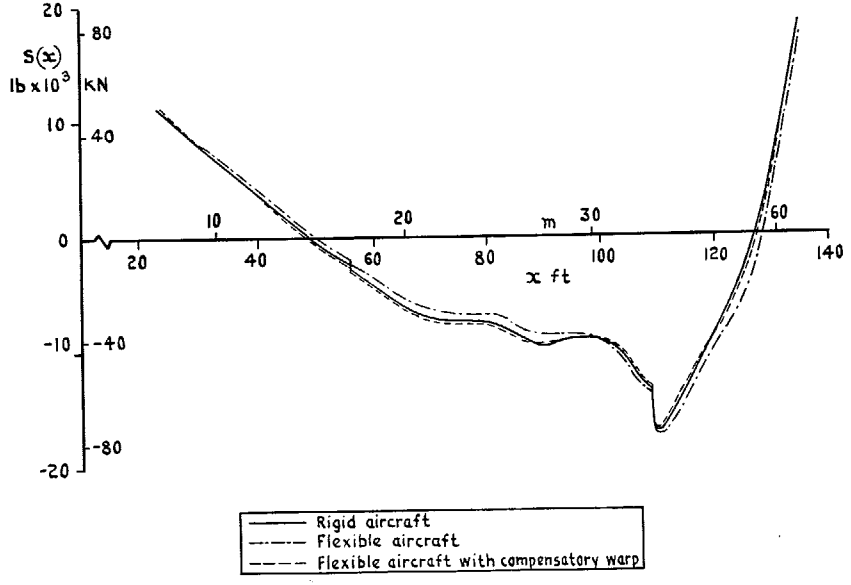

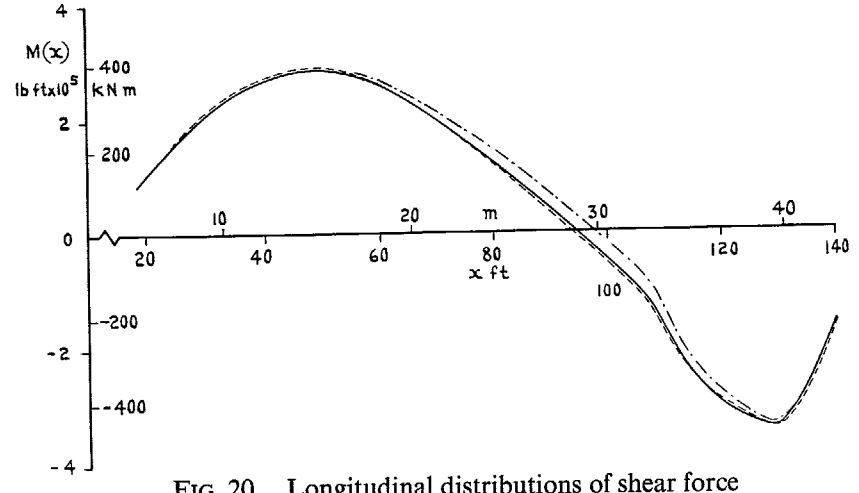

FIG. 20. Longitudinal distributions of shear force and bending moment. 'Start of cruise' fuel, $g_1 = g_2 = g_3 = 1{\cdot}0$, $Q = 670$ lb/ft^2, $n = -0{\cdot}5$.

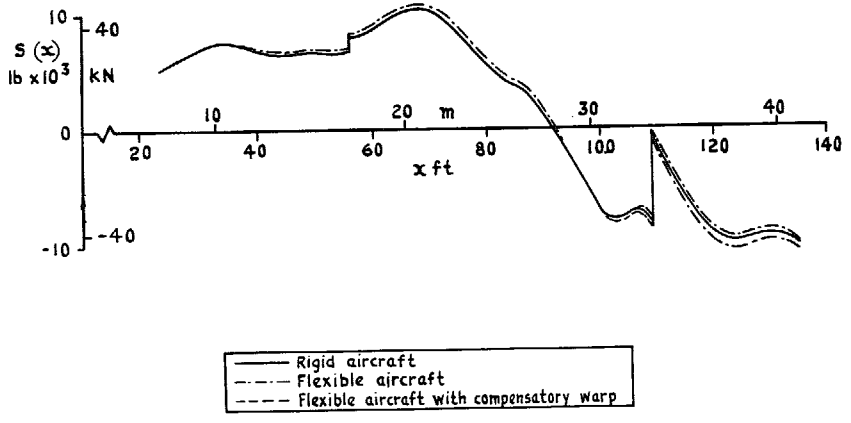

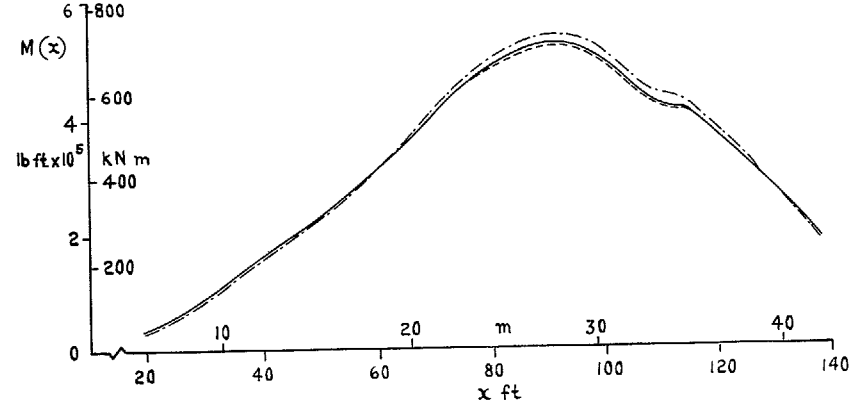

FIG. 21. Longitudinal distributions of shear force and bending moment. 'Design point' fuel, $g_1 = g_2 = g_3 = 1{\cdot}0$, $Q = 450$ lb/ft^2, $n = 1{\cdot}0$.

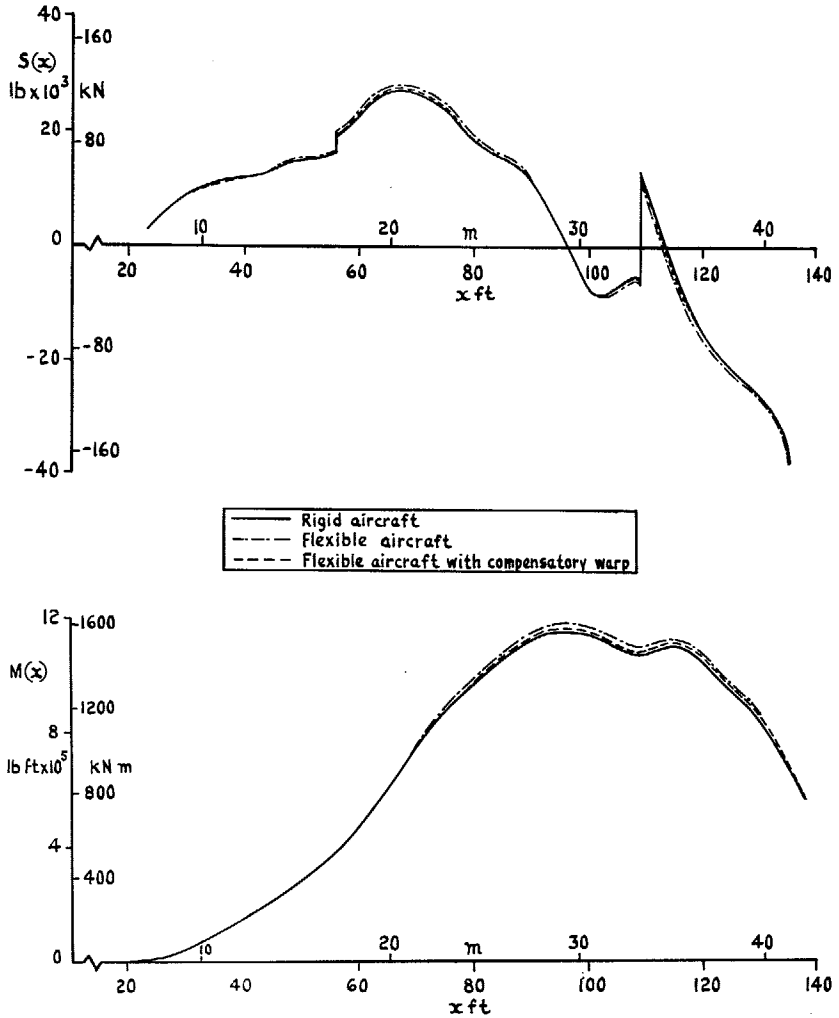

FIG. 22. Longitudinal distributions of shear force and bending moment. 'Design point' fuel, $g_1 = g_2 = g_3 = 1{\cdot}0$, $Q = 450$ lb/ft^2, $n = 2{\cdot}5$.

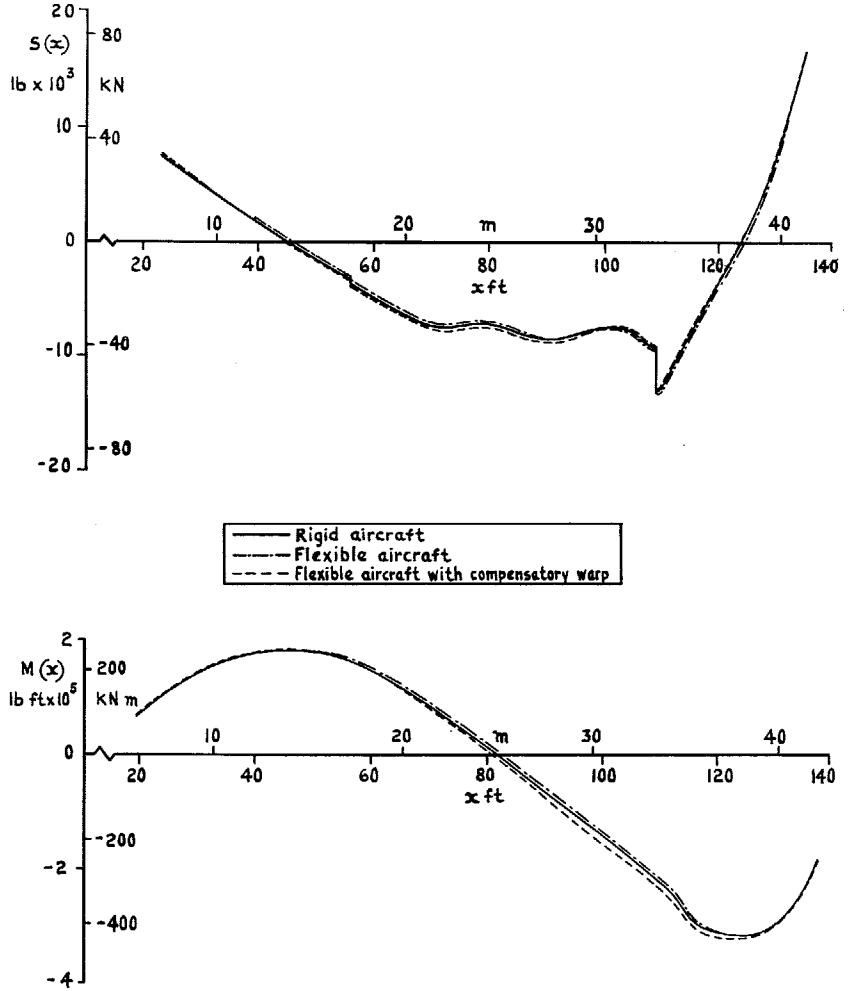

FIG. 23. Longitudinal distributions of shear force and bending moment. 'Design point' fuel, $g_1 = g_2 = g_3 = 1{\cdot}0$, $Q = 450$ lb/ft^2, $n = -0{\cdot}5$.

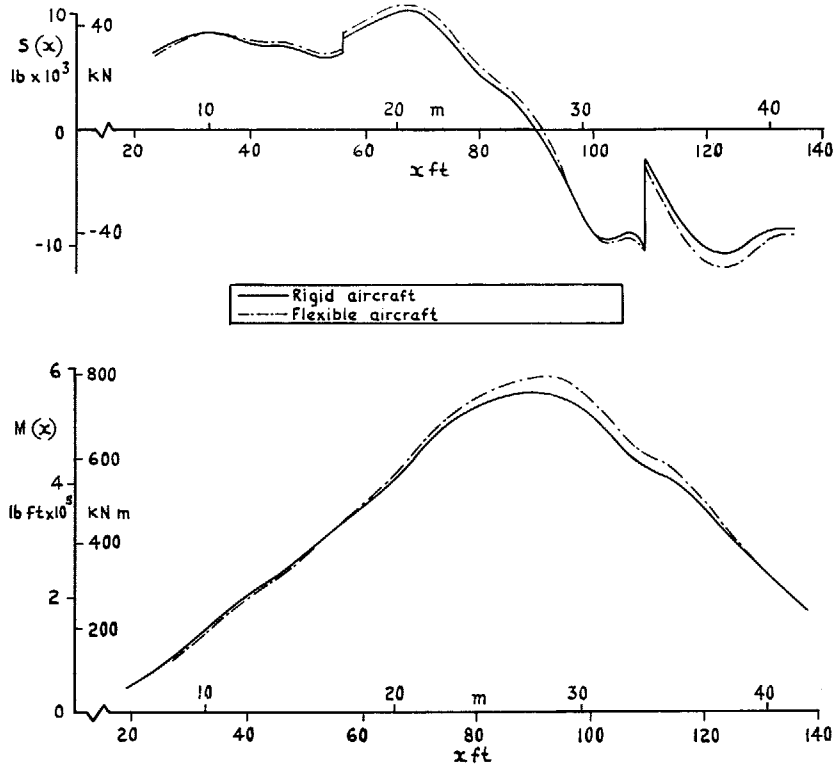

FIG. 24. Longitudinal distributions of shear force and bending moment. 'Design point' fuel, $g_1 = g_2 = g_3 = 1{\cdot}0$, $Q = 550$ lb/ft^2, $n = 1{\cdot}0$.

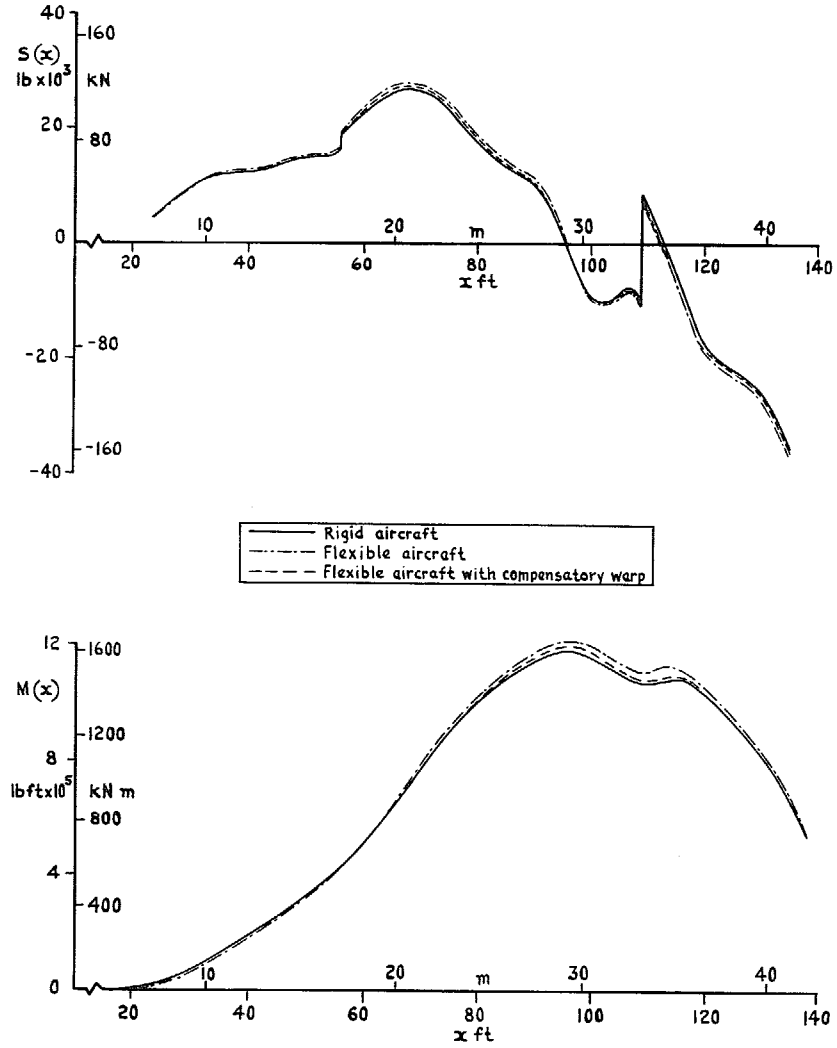

FIG. 25. Longitudinal distributions of shear force and bending moment. 'Design point' fuel, $g_1 = g_2 = g_3 = 1{\cdot}0$, $Q = 550$ lb/ft^2, $n = 2{\cdot}5$.

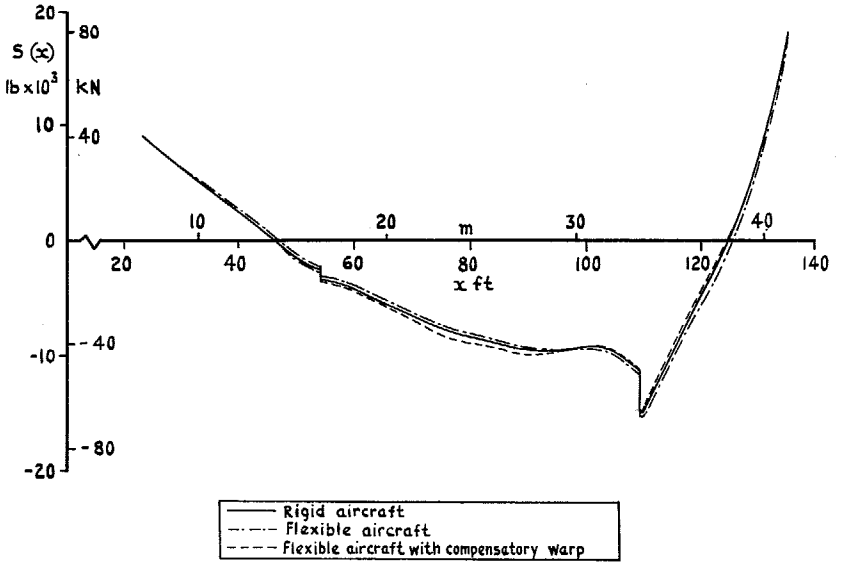

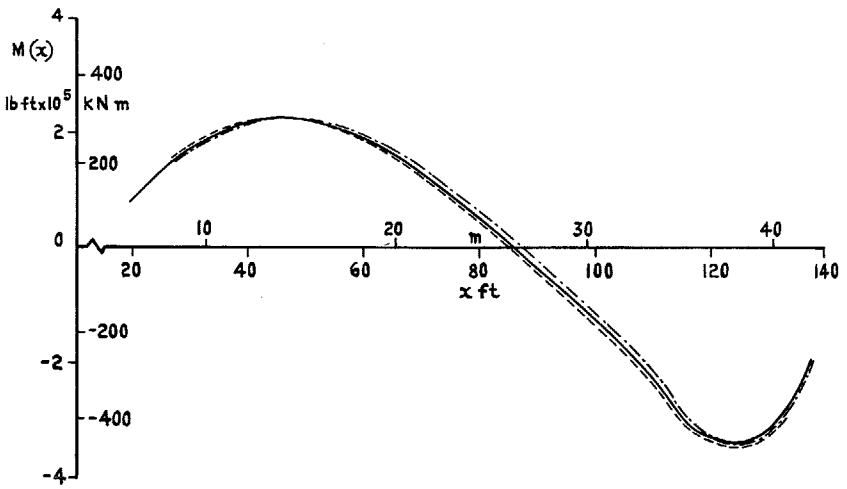

FIG. 26. Longitudinal distributions of shear force and bending moment. 'Design point' fuel, $g_1 = g_2 = g_3 = 1{\cdot}0$, $Q = 550$ lb/ft^2, $n = -0{\cdot}5$.

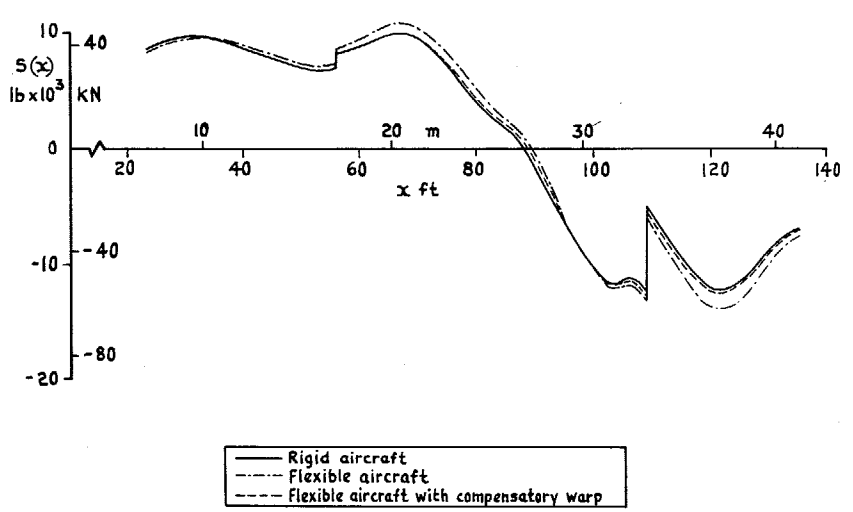

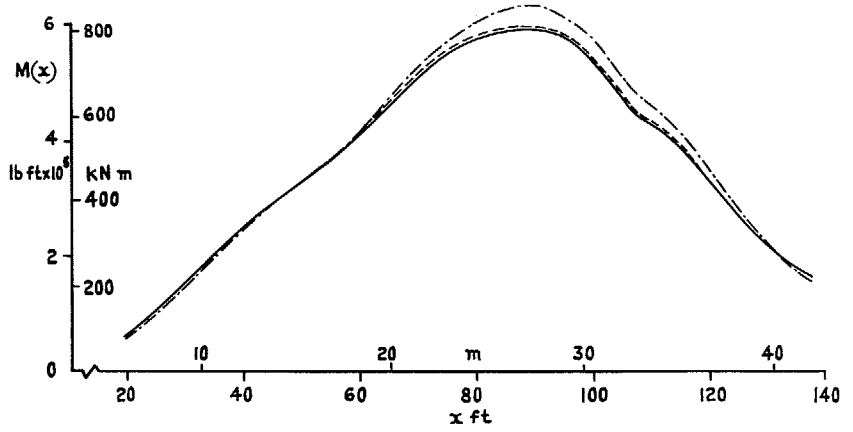

FIG. 27. Longitudinal distributions of shear force and bending moment. 'Design point' fuel, $g_1 = g_2 = g_3 = 1{\cdot}0$, $Q = 670$ lb/ft^2, $n = 1{\cdot}0$.

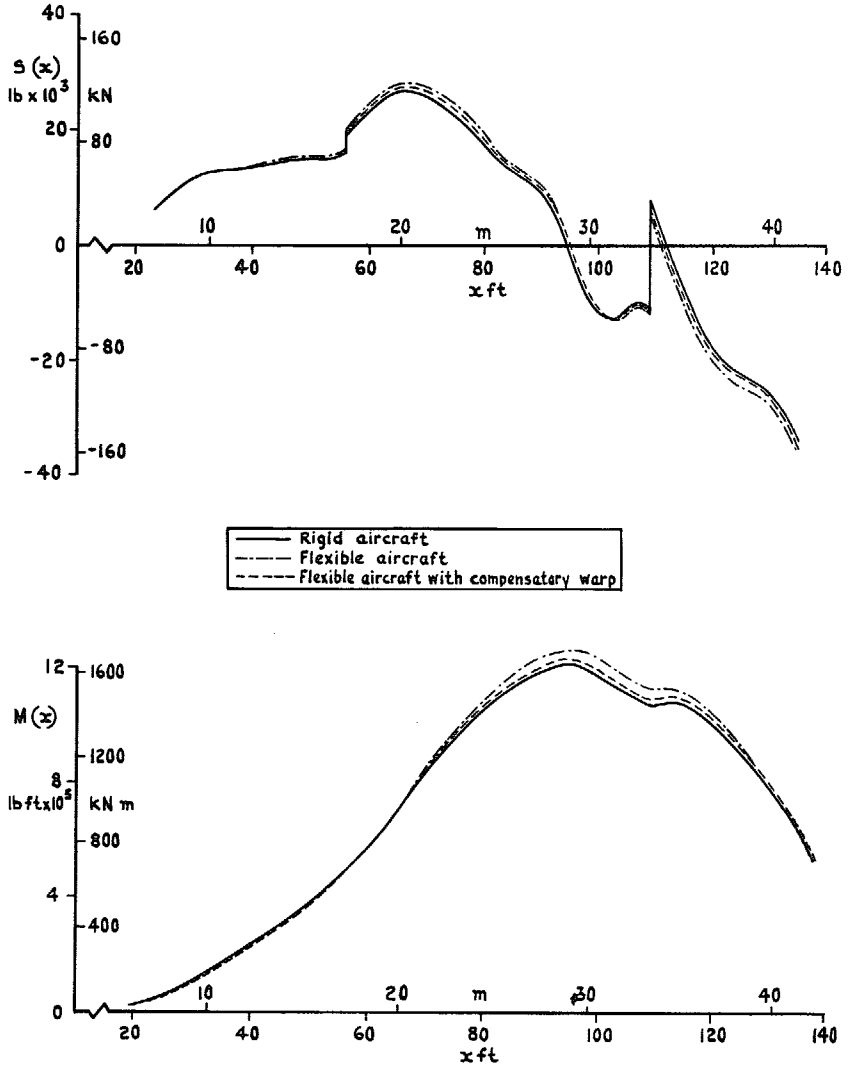

FIG. 28. Longitudinal distributions of shear force and bending moment. 'Design point' fuel, $g_1 = g_2 = g_3 = 1{\cdot}0$, $Q = 670$ lb/ft^2, $n = 2{\cdot}5$.

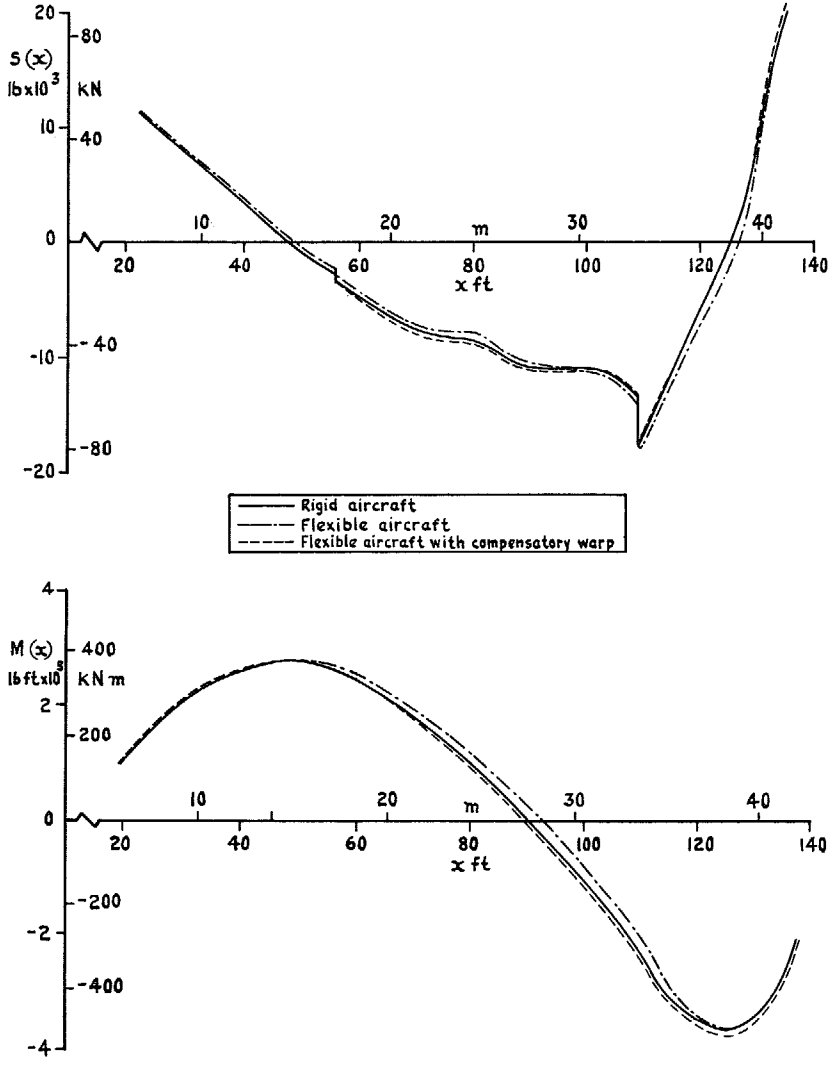

FIG. 29. Longitudinal distributions of shear force and bending moment. 'Design point' fuel, $g_1 = g_2 = g_3 = 1{\cdot}0$, $Q = 670$ lb/ft^2, $n = -0{\cdot}5$.

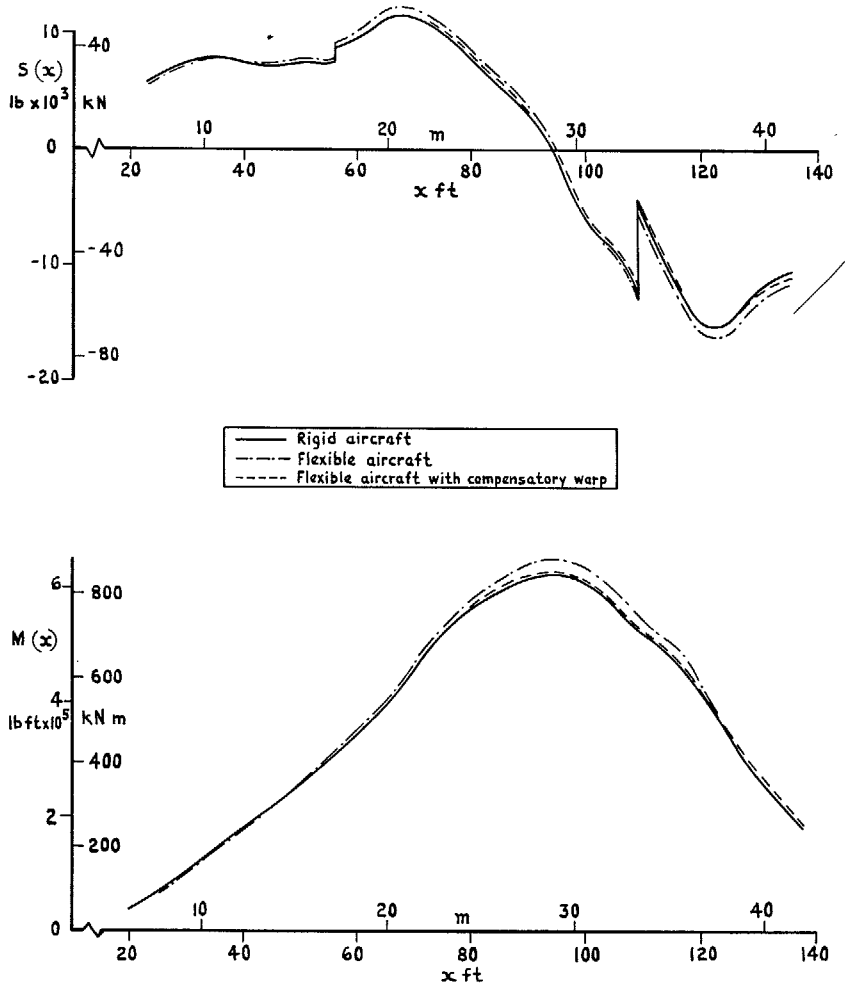

FIG. 30. Longitudinal distributions of shear force and bending moment. 'End of cruise' fuel, $g_1 = g_2 = g_3 = 1{\cdot}0$, $Q = 450$ lb/ft^2, $n = 1{\cdot}0$.

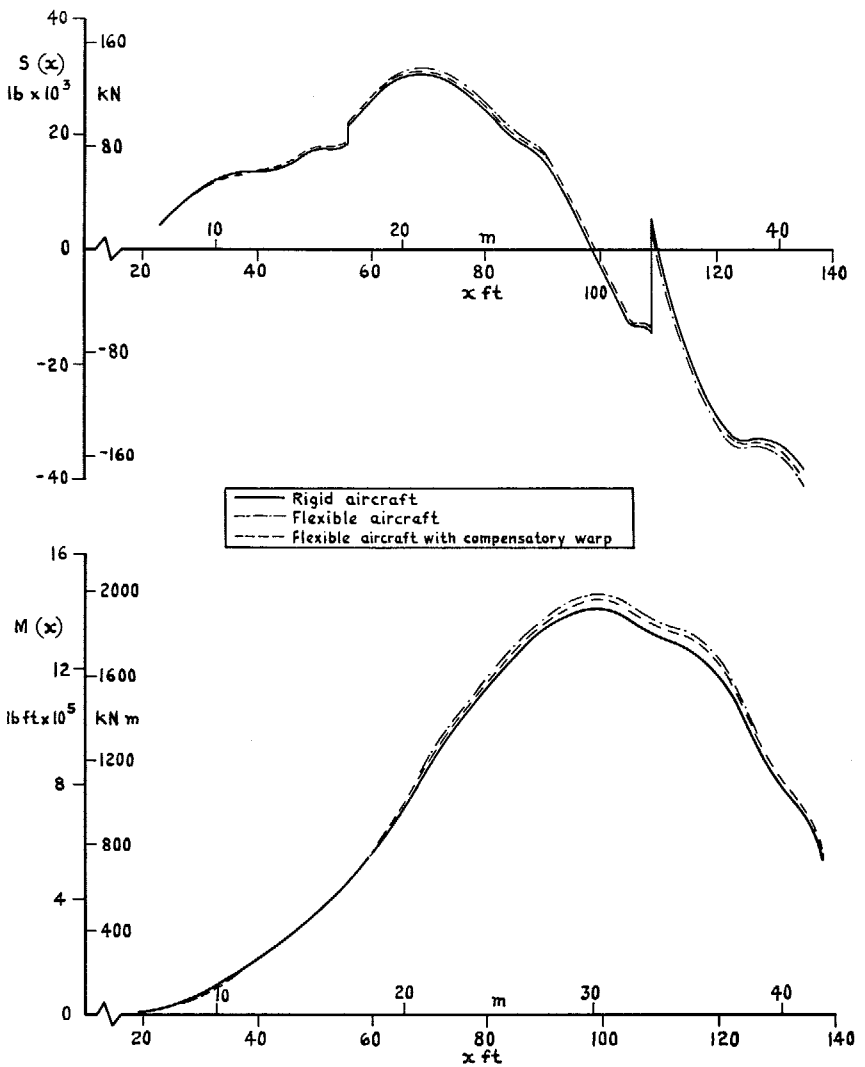

FIG. 31. Longitudinal distributions of shear force and bending moment. 'End of cruise' fuel, $g_1 = g_2 = g_3 = 1{\cdot}0$, $Q = 450$ lb/ft^2, $n = 2{\cdot}5$.

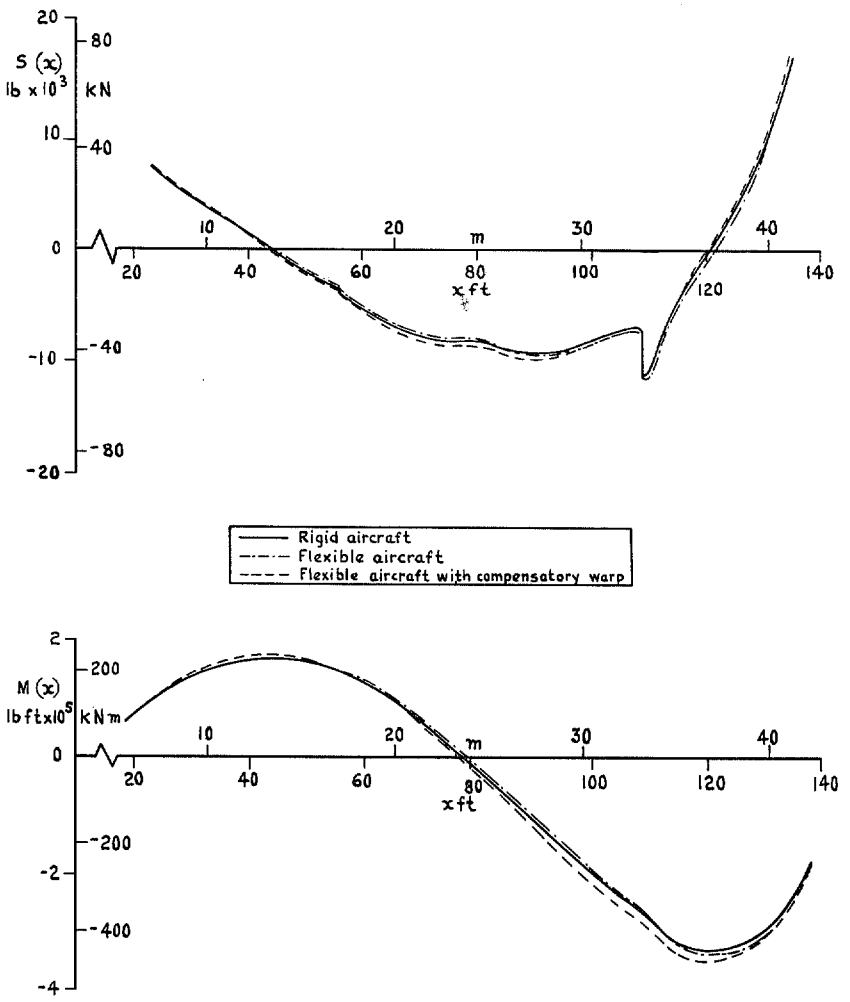

FIG. 32. Longitudinal distributions of shear force and bending moment, 'end of cruise' fuel, $g_1 = g_2 = g_3 = 1{\cdot}0, Q = 450\ \text{lb/ft}^2, n = -0{\cdot}5$.

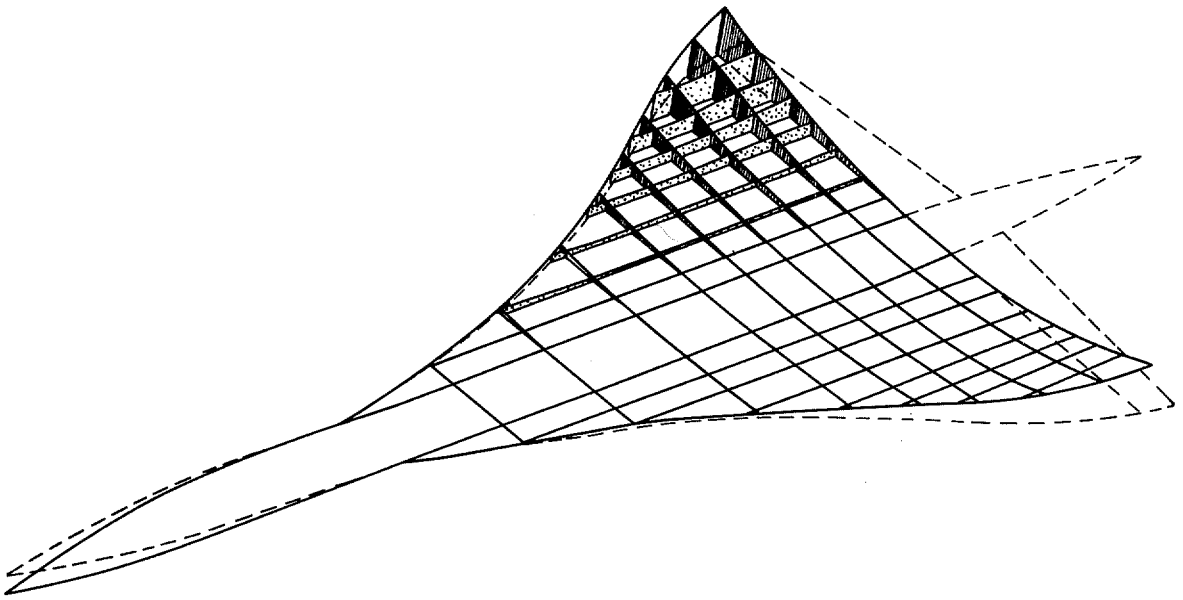

FIG. 33. Elastic warp, 'design point' fuel, $g_1 = g_2 = g_3 = 1{\cdot}0$, $Q = 550\ \text{lb/ft}^2$, $n = 1{\cdot}0$.

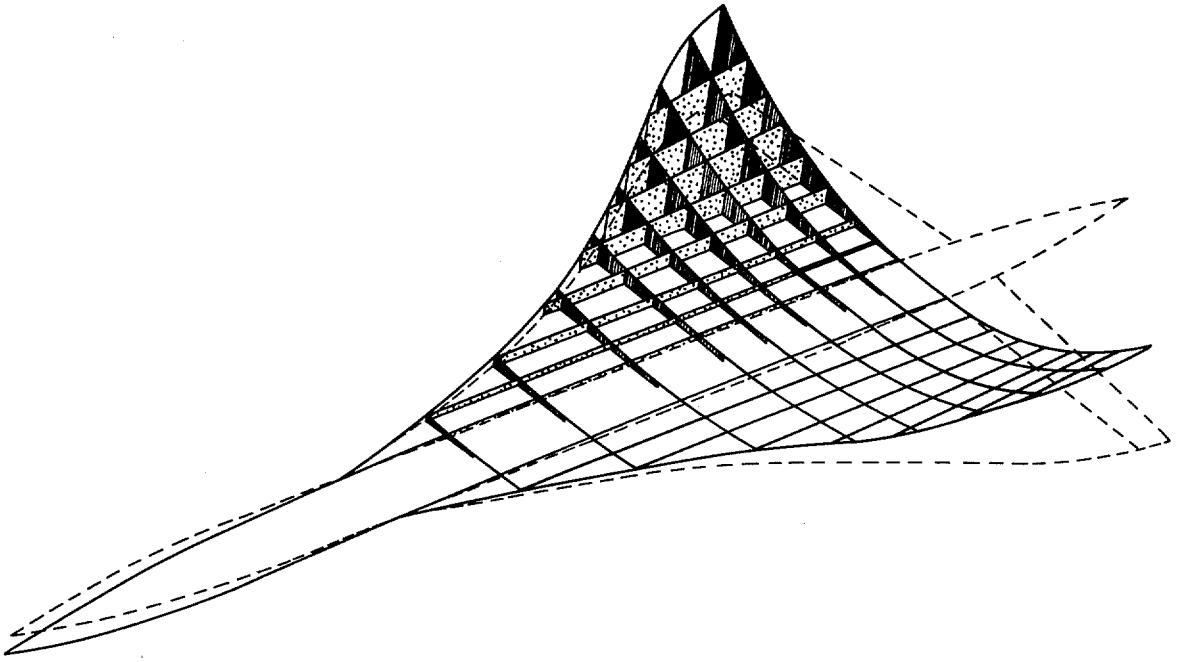

FIG. 34. Elastic warp, 'design point' fuel, $g_1 = g_2 = g_3 = 1{\cdot}0$, $Q = 550\ \text{lb/ft}^2$, $n = 2{\cdot}5$.

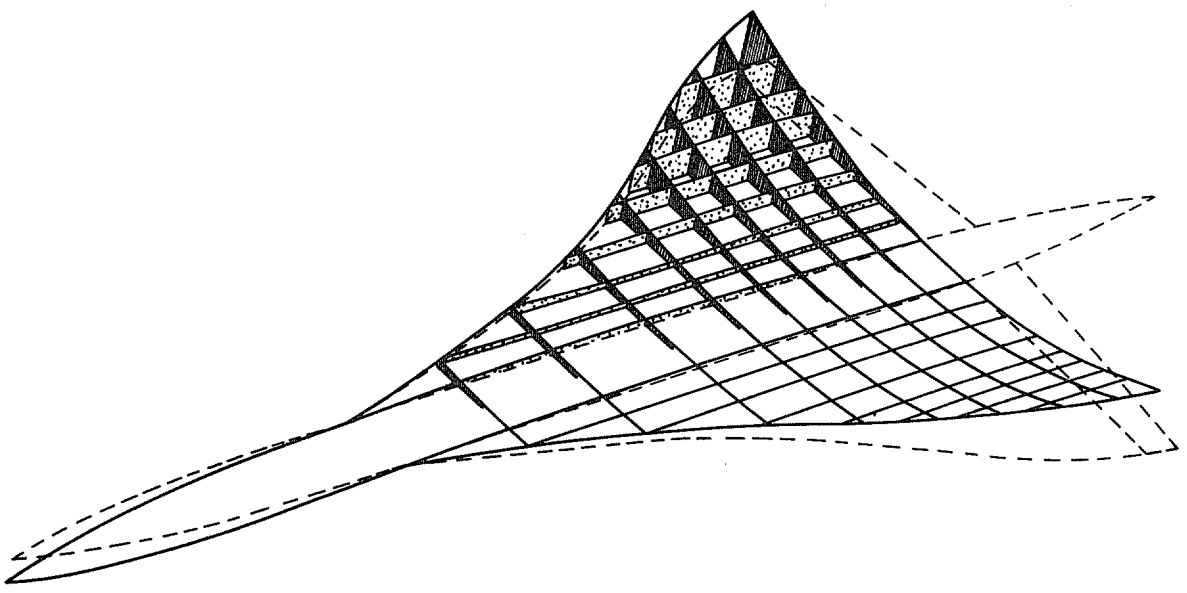

FIG. 35. Elastic warp, 'design point' fuel, $g_1 = 0, g_2 = g_3 = 1{\cdot}0, Q = 550$ lb/ft^2, $n = 2{\cdot}5$.

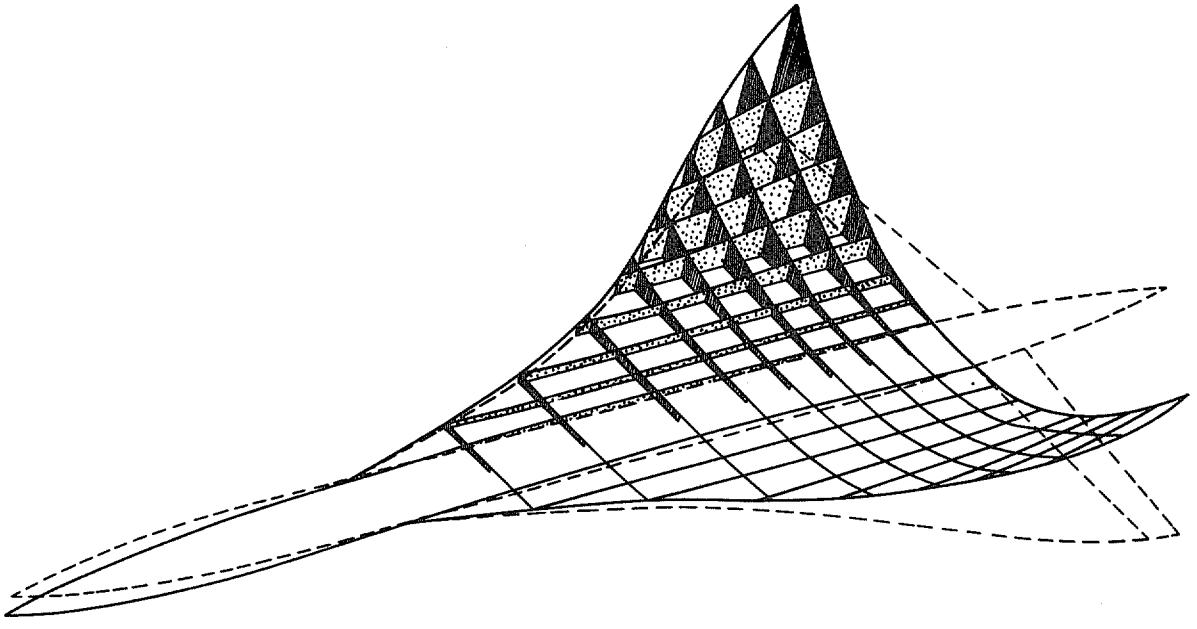

FIG. 36. Elastic warp, 'design point' fuel, $g_1 = 1{\cdot}0, g_2 = g_3 = 0, Q = 550$ lb/ft^2, $n = 2{\cdot}5$.

Printed in Wales for Her Majesty's Stationery Office by Allens Printers (Wales) Limited

Dd. 135646 K.5.

Published by
HER MAJESTY'S STATIONERY OFFICE

To be purchased from
49 High Holborn, London W.C.1
13A Castle Street, Edinburgh EH2 3AR
109 St. Mary Street, Cardiff CF1 1JW
Brazennose Street, Manchester M60 8AS
50 Fairfax Street, Bristol BS1 3DE
258 Broad Street, Birmingham 1
7 Linenhall Street, Belfast BT2 8AY
or through any bookseller

SBN 11 470232 2